A new method for reconstruction of the vertical electron density distribution in the upper ionosphere and plasmasphere

Stanimir M. Stankov, Norbert Jakowski, and Stefan Heise
Deutsches Zentrum für Luft- und Raumfahrt (DLR), Institut für Kommunikation und Navigation, Neustrelitz, Germany

Plamen Muhtarov and Ivan Kutiev
Bulgarian Academy of Sciences (BAS), Geophysical Institute, Sofia, Bulgaria

Rene Warnant
Royal Observatory of Belgium (ROB), Brussels, Belgium

Received 3 July 2002; revised 27 October 2002; accepted 13 January 2003; published 1 May 2003.

[1] Ground-based ionosphere sounding measurements alone are incapable of reliably modeling the topside electron density distribution above the F layer peak density height. Such information can be derived from Global Positioning System (GPS)-based total electron content (TEC) measurements. A novel technique is presented for retrieving the electron density height profile from three types of measurements: ionosonde (f_oF_2, f_oE, $M_{3000}F_2$, h_mf_2), TEC (GPS-based), and O^+-H^+ ion transition level. The method employs new formulae based on Chapman, sech-squared, and exponential ionosphere profilers to construct a system of equations, the solution of which system provides the unknown ion scale heights, sufficient to construct a unique electron density profile at the site of measurements. All formulae are based on the assumption of diffusive equilibrium with constant scale height for each ion species. The presented technique is most suitable for middle- and high-geomagnetic latitudes and possible applications include: development, evaluation, and improvement of theoretical and empirical ionospheric models, development of similar reconstruction methods utilizing low-earth-orbiting satellite measurements of TEC, operational reconstruction of the electron density on a real-time basis, etc. *INDEX TERMS:* 2447 Ionosphere: Modeling and forecasting; 2481 Ionosphere: Topside ionosphere; 2494 Ionosphere: Instruments and techniques; 7819 Space Plasma Physics: Experimental and mathematical techniques; 7843 Space Plasma Physics: Numerical simulation studies; *KEYWORDS:* reconstruction technique, electron profile, transition level, ionosonde, GPS, TEC

Citation: Stankov, S. M., N. Jakowski, S. Heise, P. Muhtarov, I. Kutiev, and R. Warnant, A new method for reconstruction of the vertical electron density distribution in the upper ionosphere and plasmasphere, *J. Geophys. Res.*, *108*(A5), 1164, doi:10.1029/2002JA009570, 2003.

1. Introduction

[2] The knowledge of the electron density distribution in the Earth's topside ionosphere and plasmasphere is important from several aspects, such as estimation and correction of propagation delays in the Global Navigation Satellite System (GNSS), ionospheric storm studies, ion composition studies, space-weather effects on telecommunications, etc.

[3] The traditional ground-based vertical incidence sounding (ionosonde) measurements are sufficient for a precise determination of the bottom-side electron density profile. However, the ground-based ionosonde measurements alone are incapable of delivering information about the topside electron profile (above h_mf_2). A typical way of "solving" the problem, adopted in the modern digital ionosondes [*Reinisch*, 1996a, 1996b] is to use a Chapman layer [*Banks and Kockarts*, 1973]. A nice feature of this Chapman profiler is that it needs only the peak density and height values to calculate the topside distribution. However, it demonstrates some disadvantages associated first with the use of constant plasma scale height determined from the density distribution around the peak, and second, with the fact that the constructed profile is not tied to any additional measurements.

[4] During the years, the researchers have developed and used other means to gather information on the upper ionosphere and plasmasphere, such as: coherent scatter radar observations of underdense electron density irregularities [*Booker*, 1956; *Greenwald*, 1996], incoherent scatter radar probing [*Bowles*, 1958; *Gordon*, 1958; *Farley*, 1996], observations using topside sounders onboard satellites [*Franklin and Maclean*, 1969; *Reinisch et al.*, 2001], in situ rocket and satellite observations [*Pfaff*, 1996], tomography [*Austen et al.*, 1988; *Leitinger*, 1996b], and occultation measurements [*Phinney and Anderson*, 1973; *Leitinger*,

0148-0227/03/2002JA009570$09.00

1996b]. There is no universal method; each type has advantages as well as shortcomings.

[5] The total electron content (TEC) is one of the most important quantitative characteristics of the Earth's ionosphere and plasmasphere. The (vertical) TEC is defined as the integral of the electron density from the ground height up to the ceiling height, i.e., the height of the transmitting satellite or infinity [*Leitinger*, 1996a]. The electron density above approximately 2000 km contributes little (less than 5%) to the integrated electron content and above the mean height of the plasmapause (25,000 km) the contribution is negligible. All modern TEC measuring systems rely on the observation of signal phase differences or on pulse travel time and pulse shape measurements based on geostationary and orbiting satellites. A standard way of measuring TEC is to use ground-based receiver processing signals from: satellites on geostationary orbits, like ATS-6, SIRIO; polar orbiting satellites, like the US Navy Navigation Satellite System (NNSS), the Russian Global Navigation Satellite System (GLONASS) satellites; and the Global Positioning System (GPS) satellites. The development of the GPS has also opened new opportunities to investigate the ionosphere and plasmasphere on a global scale [*Davies and Hartmann*, 1997].

[6] The purpose of this paper is to present a novel approach to the solution of a long-standing problem: the reconstruction of the electron density distribution from the TEC. Proposed is a new technique for reconstructing the topside electron density profile from the three basic types of measurements: ground-based vertical incidence sounding (ionosonde) data, GPS-based TEC measurements, and empirical values of the upper (O^+-H^+) ion transition height. The aim is to construct a unique height profile of the electron density closely matching the existing conditions at the time of measurements (Figure 1). The ionosonde measurements are important for providing the bottom-side shape of the electron profile including N_mF_2 and h_mF_2. Even if we know the F layer peak density and height, we cannot determine the topside electron distribution because the topside plasma scale height is unknown. The upper transition level (UTL) (if available) is the reference point we need to calculate the plasma scale height. Then, assuming an adequate topside density distribution law the profile can be tied to the F layer peak height and the O^+-H^+ transition height. The fulfillment of the most important quantitative requirement should still be observed, i.e., the calculated TEC (sum total of the integrated bottom side and topside electron density) should equal the measured TEC.

[7] This paper is structured in the following way. First, a general formulation of the problem and overview of the reconstruction method is presented. Second, the most important ionosphere "profilers" (Chapman, exponential, sech-squared, and parabolic) are examined in detail and the corresponding reconstruction formulae are deduced. Third, all required input parameters for this reconstruction are presented: GPS TEC, ionosonde, and O^+-H^+ ion transition height data. Next, important evaluation results are provided in order to determine the most suitable profiler for given geophysical conditions. Evaluations involve satellite in situ observations and theoretical estimations based on calculations using same scale heights and TEC values. In the last part, possible applications of the reconstruction technique are discussed, such as the use of TEC measurements onboard Low Earth-Orbiting (LEO) satellites for profile reconstruction purposes, two- and three-dimensional electron density distribution, and the operational reconstruction on a real-time basis.

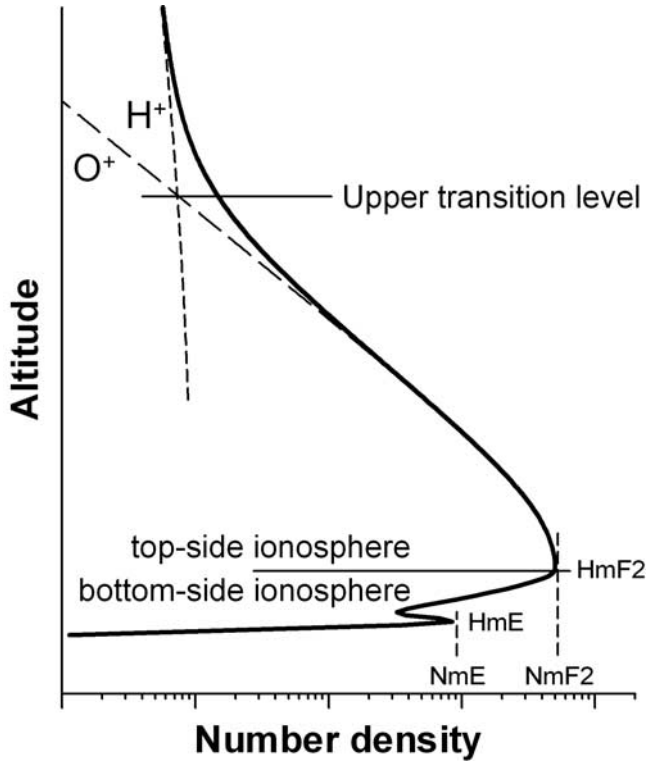

Figure 1. Ion and electron density profile characteristics.

2. Mathematical Formulation: General Problem Definition and Overview of the Reconstruction Method

[8] The problem can be stated in the following way. Let us suppose that at a given location and at a given time, we have the main ground ionosonde data and GPS-based TEC measurements available. The task is to construct a vertical electron profile, which most adequately represents the current geophysical conditions (Figure 1). There are two aspects of difficulty: finding the suitable ionospheric "profiler" and calculating the plasma scale height(s). The task is complicated because the TEC is an integral quantity providing no details of the topside profile shape. Such details can be provided by considering additional "shape factors" like ion composition, plasma fluxes, etc. For example, the previous attempts to model the topside electron distribution involved direct modeling of the electron density. Here we are modeling the individual ion densities and from them the electron density is derived. Such treatment allows the inclusion of another important "shape factor" like the O^+-H^+ ion transition level. The O^+-H^+ ion transition level, also known as the UTL, is the height where the concentration of the O^+ ions equals that of the H^+ ions. The effect on the electron profile is that at this altitude, the gradient (of the vertical distribution) generally increases sharply because of the different scale heights of the ingredient O^+ and H^+ ion profiles, and

thus denoting the beginning of the plasmasphere. It is possible to obtain UTL values from empirical models [*Bilitza et al.*, 1993; *Kutiev et al.*, 1994].

[9] Given the type of the topside ionosphere profiler, an ion concentration profile is uniquely identified if the ion concentration at the h_mF_2 (N_{mi}) and the topside ion scale height (H_i) are both known. Therefore if we consider the topside ionosphere consisting of the two major ions (oxygen and hydrogen), we need to know four parameters to construct the topside electron profiles: the oxygen topside scale height (H_{O^+}), oxygen concentration at h_mF_2 (N_{mO^+}) the hydrogen topside scale height (H_{H^+}), and hydrogen concentration at h_mF_2 (N_{mH^+}). These unknowns require a system of four equations to be constructed in order to find a unique solution. Considering the above available information, let the topside ''ionosphere profile'' be a function $\Im$ (concentration) depending on height (h) and the ionosonde parameters, transition level, and ion scale height, i.e.,

$$\Im_i(h) = \Im_i(H_i, N_{mi}, h_mF_2; h). \tag{1}$$

Therefore the height profile of the electron density is calculated from the following reconstruction formula:

$$\Im_e(h) = \Im_{O^+}(H_{O^+}, N_{mO^+}, h_mF_2; h) + \Im_{H^+}(H_{H^+}, N_{mH^+}, h_mF_2; h). \tag{2}$$

For determination of the above-mentioned unknowns (H_{O^+}, N_{mO^+}, H_{H^+}, N_{mH^+}), the following system of equations is proposed:

$$N_{mO^+} + N_{mH^+} = N_m, \tag{3}$$

$$H_{H^+} = (\mu_{O^+}/\mu_{H^+})\xi H_{O^+}, \tag{4}$$

$$\mathbf{\Phi}_t = \aleph_{O^+}(H_{O^+}, N_{mO^+}, h_mF_2) + \aleph_{H^+}(H_{H^+}, N_{mH^+}, h_mF_2), \tag{5}$$

$$\Im_{O^+}(H_{O^+}, N_{mO^+}, h_mF_2; h_{tr}) = \Im_{H^+}(H_{H^+}, N_{mH^+}, h_mF_2; h_{tr}), \tag{6}$$

where N_m is the F_2 layer peak electron density(N_mF_2), μ_{O^+} is the O^+ ion mass, μ_{H^+} is the H^+ ion mass, ξ is the vertical scale height corrector, $\xi = \sin[\text{arctg}(2tg\varphi)]$, φ being the latitude, h_{tr} is the O^+-H^+ ion transition level, $\mathbf{\Phi}_t$ is the measured topside TEC (above h_mF_2), $\aleph_{mO^+}$ is the integrated topside O^+ ion concentration, and $\aleph_{mH^+}$ is the integrated topside H^+ ion concentration.

[10] The first system equation, equation (3), represents the principle of plasma quasineutrality, applied to the topside (at and above h_mF_2) ionosphere and based on the assumption that the O^+ and H^+ ions are the major ions.

[11] Equation (4) represents the relation between both scale heights in vertical direction. However, the plasma diffusion occurs predominantly along the geomagnetic field lines. Along a geomagnetic field line, and under isotropic conditions, the H^+ scale height will be approximately 16 times larger than the O^+ scale height, following the scale height definition ($H_i = kT_i/m_ig$) and the assumption that the ion temperatures are equal. In vertical direction, the ratio 1:16 is no longer preserved and depends mainly on the latitude. Hence a correction factor should be applied, and the sole purpose of using such factor is to map the scale height (along the field line) onto the vertical axis, z, which in effect will redistribute the plasma density in height direction. From simple geometrical considerations, it follows that $dz = \sin \boldsymbol{I} ds$ where dz is the differential element along the vertical, ds is the differential element along the field line, and $\boldsymbol{I}$ is the inclination. There are two common sources for the inclination: measured values (inclination at an observing station) or values calculated from a spherical harmonics expansion of the geomagnetic field. Sometimes the inclination in the ionosphere (e.g., at the F_2 peak height, H_mF_2) is taken instead of the inclination at the ground. The construction here simply adopts the relation between magnetic latitude and inclination (dip angle) for a dipole leading to the equation $\tan\varphi = 1/2 \tan \boldsymbol{I}$, where φ is the dip-latitude [*Chapman*, 1963]. Finally, the correction factor is found to be $\xi = \sin[\text{arc}tg(2tg\varphi)]$.

[12] Equation (5) is obtained after integrating the proposed ''reconstruction'' formula (2) from h_mF_2 to infinity. The integration of the right-hand side is difficult and depends on the type of the ionospheric profiler used. Details of the integration utilizing the most frequently used analytical profilers are provided in the next part of this paper. The topside part of the TEC, $\mathbf{\Phi}_t$, is obtained as the difference between the TEC total measured value, $\mathbf{\Phi}$, and the bottomside part (below h_mF_2), $\mathbf{\Phi}_b$. For this purpose, the bottom-side electron profile is first constructed using the available ground ionosonde measurements: the bottom-side profile is presented as a composition of two (F_2 and E) Epstein-type layers by using f_oF_2, f_oE, $m_{3000}F_2$, and h_mF_2 [*Di Giovanni and Radicella*, 1990]. Once the bottom-side profile is obtained, the corresponding bottom-side electron content, $\mathbf{\Phi}_b$, is calculated. Having $\mathbf{\Phi}$ and $\mathbf{\Phi}_b$, the topside part is $\mathbf{\Phi}_t = \mathbf{\Phi} - \mathbf{\Phi}_b$, used in equation (5).

[13] The last system equation, equation (6), summarizes the fact that the hydrogen and oxygen ion densities are equal at the O^+-H^+ transition level (h_{tr}). This equation fastens all the information that is provided to realize the proposed reconstruction technique.

[14] The equation system (3)–(6) is solved by excluding the unknowns from the first three equations and replacing them in the last equation, equation (6). The resulting transcendental equation (with unknown H_{O^+}) is solved using dichotomy method for finding the root. Having the oxygen scale height, the rest of the unknowns are found from formulae (3)–(5). The topside electron profile is then easy to reconstruct from formula (2).

3. Analytical Ionospheric Profilers for Use in the Reconstruction

[15] In this part, more details will be provided on the reconstruction method and new formulae will be deduced using the most suitable (in view of both physical adequacy and numerical handling) analytical models: the exponential, sech-squared, and Chapman layers [*Davies*, 1996; *Stankov*, 2002a]. The applicability of the parabolic layer is also discussed. All formulae are based on the assumption of

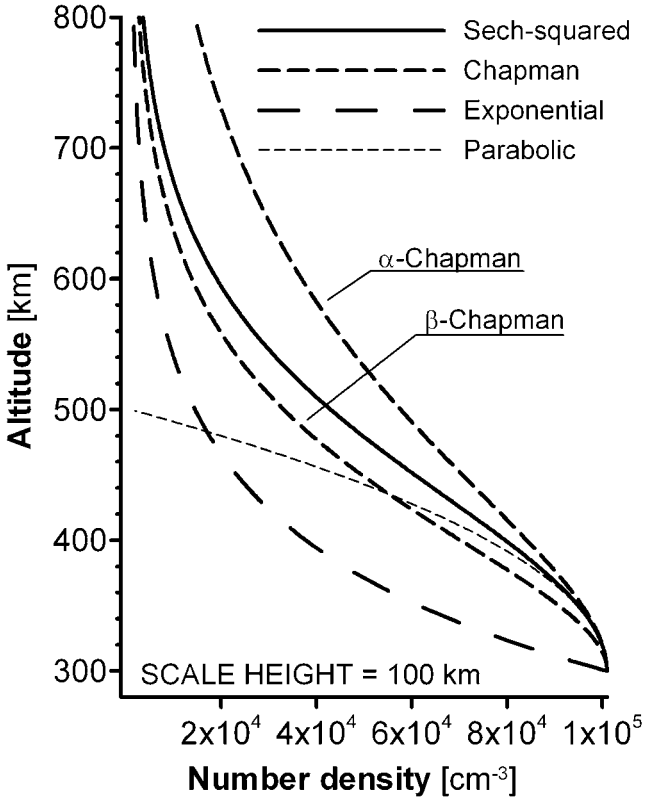

Figure 2. Comparison between vertical electron density profiles obtained with basic analytical models for a given scale height of 100 km.

diffusive equilibrium (Appendix A) with constant scale height for each ion species. Typical topside density distributions for the above mentioned analytical models are presented in Figure 2.

[16] The topside electron content is the integral of the electron content from the F_2 layer peak density height, h_m, up to the ceiling height h_c (the height of the transmitting satellite or infinity), i.e.,

$$\Phi(h_m, h_c) = \int_{hm}^{hc} N_e(h)dh = \int_{hm}^{hc} N_{O^+}(h)dh + \int_{hm}^{hc} N_{H^+}(h)dh, \quad (7)$$

and both integrals on the right-hand side are solved in the same way, which will be described below for each profiler. Notice that the height h_c is practically infinity in the case of GPS measurements since the electron density above the mean height of the plasmapause contributes a negligible quantity to the integrated electron content.

3.1. Sech-Squared Layer

[17] The sech-squared (Epstein) layer is defined as:

$$N_i(h) = N_i(h_m)\mathrm{sech}^2\left(\frac{h-h_m}{2H_i}\right), \quad (8)$$

where $N_i(h)$ is the ion (O^+ or H^+) density at height h, H_i is the ion (O^+ or H^+) scale height, sech(h) = 1/cos (h), cosh(x) = 0.5 (exp(h) + exp(-h)).

[18] The integrals in formula (7) are solved by applying three successive substitutions (Appendix B) leading to

$$\Phi_t = 2H_{O^+}N_{O^+}(h_m) + 2H_{H^+}N_{H^+}(h_m). \quad (9)$$

Considering the fact that at the UTL (h_{tr}) the oxygen and hydrogen ion densities are equal, the transcendental equation then reads [*Stankov and Muhtarov*, 2001; *Stankov et al.*, 2002]:

$$\left(\frac{16\xi}{(16\xi-1)}N_m - \frac{1}{2(16\xi-1)H_{O^+}}\Phi_t\right)\mathrm{sech}^2\left(\frac{h_{tr}-h_m}{2H_{O^+}}\right) - \left(\frac{1}{2(16\xi-1)H_{O^+}}\Phi_t - \frac{1}{(16\xi-1)}N_m\right)\mathrm{sech}^2\left(\frac{h_{tr}-h_m}{32\xi H_{O^+}}\right). \quad (10)$$

The only unknown variable in the above transcendental equation is the oxygen ion scale height, which is obtained after numerically solving the equation. It is assumed that the ionosphere is isotropic, therefore the H^+ scale height will be approximately 16 times larger than the O^+ scale height. The correction factor ξ represents the change from magnetic field line direction to vertical direction, discussed in section 2 of this paper.

3.2. Exponential Layer

[19] The Exponential layer is defined as:

$$N_i(h) = N_i(h_m)\exp\left(-\frac{h-h_m}{H_i}\right), \quad (11)$$

where $N_i(h)$ is the density at height h, H_i (positive) is the ion scale height. For the exponential profiler the topside electron content calculations (see Appendix C) lead to

$$\phi_t = H_{O^+}N_{O^+}(h_m) + H_{H^+}N_{H^+}(h_m). \quad (12)$$

The corresponding equation for obtaining the scale height is now:

$$\left(\frac{16\xi}{(16\xi-1)}N_m - \frac{1}{(16\xi-1)H_{O^+}}\Phi_t\right)\exp\left(-\frac{h_{tr}-h_m}{H_{O^+}}\right) - \left(\frac{1}{(16\xi-1)H_{O^+}}\Phi_t - \frac{1}{(16\xi-1)}N_m\right)\exp\left(-\frac{h_{tr}-h_m}{16\xi H_{O^+}}\right) = 0. \quad (13)$$

3.3. Chapman Layer

[20] The general form of the Chapman layer is

$$N(h) = N(h_m)\exp\left\{c\left[1 - \frac{h-h_m}{H} - \exp\left(-\frac{h-h_m}{H}\right)\right]\right\}, \quad (14)$$

where h_m is the peak density height and H is the scale height, c is the type coefficient. This model has two distinct formulations: the so-called α-Chapman layer (c = 0.5) and β-Chapman layer (c = 1), depending on assumptions related to the electron recombination theory

[*Hargreaves*, 1992]. The α-Chapman layer assumes that the electrons recombine directly with positive ions and that no negative ions are present, i.e., $X^+ + e \rightarrow X$, and the lost rate is then $L = \alpha N^2$ where α is the recombination coefficient. In the β-Chapman formulation, the assumption is that the electron loss is through attachment to neutral particles, i.e., $X + e \rightarrow X^-$ with linear loss rate $L = \beta N$, where β is the attachment coefficient. As height increases, the behavior changes from α to β type at a height where $\beta = \alpha N$.

[21] For the α-Chapman layer, the density at a given height is

$$N(h) = N(h_m)\exp\left\{\frac{1}{2}\left[1 - \frac{h-h_m}{H} - \exp\left(-\frac{h-h_m}{H}\right)\right]\right\}. \quad (15)$$

After applying substitutions, the integration of the α-Chapman function yields (Appendix D):

$$\Phi_t = 2.821 H_{O^+} N_{O^+}(h_m) + 2.821 H_{H^+} N_{H^+}(h_m) \quad (16)$$

and the equation for determining the O^+ scale height is

$$\begin{aligned}&\left(\frac{16\xi}{(16\xi-1)}N_m - \frac{1}{2.821(16\xi-1)H_{O^+}}\Phi_t\right)\\ &\cdot\exp\left(1 - \frac{h_{tr}-h_m}{H_{O^+}} - \exp\left(-\frac{h_{tr}-h_m}{H_{O^+}}\right)\right)\\ &-\left(\frac{1}{2.821(16\xi-1)H_{O^+}}\Phi_t - \frac{1}{(16\xi-1)}N_m\right)\\ &\cdot\exp\left(1 - \frac{h_{tr}-h_m}{16\xi H_{O^+}} - \exp\left(-\frac{h_{tr}-h_m}{16\xi H_{O^+}}\right)\right) = 0.\end{aligned} \quad (17)$$

Similarly, for the β-Chapman layer the density at a given height is

$$N(h) = N(h_m)\exp\left\{\left[1 - \frac{h-h_m}{H} - \exp\left(-\frac{h-h_m}{H}\right)\right]\right\}. \quad (18)$$

Then, the topside electron content is (Appendix D):

$$\Phi_t = 1.718 H_{O^+} N_{O^+}(h_m) + 1.718 H_{H^+} N_{H^+}(h_m) \quad (19)$$

and the equation for determining the O^+ scale height is

$$\begin{aligned}&\left(\frac{16\xi}{(16\xi-1)}N_m - \frac{1}{1.718(16\xi-1)H_{O^+}}\Phi_t\right)\\ &\cdot\exp\left(1 - \frac{h_{tr}-h_m}{H_{O^+}} - \exp\left(-\frac{h_{tr}-h_m}{H_{O^+}}\right)\right)\\ &-\left(\frac{1}{1.718(16\xi-1)H_{O^+}}\Phi_t - \frac{1}{(16\xi-1)}N_m\right)\\ &\cdot\exp\left(1 - \frac{h_{tr}-h_m}{16\xi H_{O^+}} - \exp\left(-\frac{h_{tr}-h_m}{16\xi H_{O^+}}\right)\right) = 0.\end{aligned} \quad (20)$$

3.4. Parabolic Layer

[22] The parabolic layer is defined as $N(h) = N(h_m)\{1 - [(h - h_m)/2H]^2\}$, where typical values of H for the F_2 region lie in the range of 25–50 km [*Davies*, 1996]. This layer is suitable for modeling the profile near h_mF_2 and is helpful when extracting information from the satellite data. It is also good for constructing composite ionospheric models [*Rawer*, 1988]. However, as a reconstruction tool, used separately, it is certainly not appropriate.

4. Measurement Data for Use in the Reconstruction (Required Input)

4.1. TEC Measurements

[23] After determining the TEC along a number of ray paths by using a special calibration technique for the ionospheric delay of GPS signals [*Sardon et al.*, 1994], the slant TEC is mapped to the vertical by using a single-layer approximation for the ionosphere at h_{sp} = 400 km height. Using the GPS ground stations of the European IGS network, about 60–100 TEC data points are available for reconstructing TEC maps over the area $20°W \leq \lambda \leq 40°E$; $32.5°N \leq \varphi \leq 70°N$. To ensure a high reliability of the TEC maps also in case of only a few measurements or at greater distances from measuring points, the measured data are combined with the empirical TEC model NTCM2 [*Jakowski*, 1996]. For each grid point value (spacing is 2.5°/5° in latitude/longitude) a weighting process between nearest measured values and model values is carried out. The achieved accuracy for TEC is on the order of $2–3 \times 10^{16}$ m^{-2} [*Jakowski et al.*, 1996]. To derive TEC over the ionosonde stations considered in this study, a linear interpolation algorithm within the corresponding grid pixel is applied.

4.2. Vertical Ionospheric Sounding (Ionosonde) Measurements

[24] The information about the bottom-side part of the profile and the electron peak density and peak height is taken from ionosonde measurements; required ionosonde parameters are the F_2 layer critical frequency (foF_2), the propagation factor ($M_{3000}F_2$), and the E layer critical frequency (foE). The F_2 layer peak height is estimated using the expression [*Dudeney*, 1983]:

$$\begin{aligned}h_mF_2 &= -176 + 1470\\ &\cdot\frac{M_{3000}F_2\left\{\left[0.0196(M_{3000}F_2)^2 + 1\right]/\left[1.296(M_{3000}F_2)^2 - 1\right]\right\}^{1/2}}{M_{3000}F_2 - 0.012 + 0.253/(f_oF_2/f_oE - 1.215)}.\end{aligned} \quad (21)$$

The bottom-side thickness, B_{bot}, is calculated by [*Di Giovanni and Radicella*, 1990]:

$$B_{bot} = 0.385 N_m F_2 (dN/dh)^{-1}_{\max} \quad (22)$$

where $(dN/dh)_{\max}$ is the value of the gradient of $N_e(h)$ at the base of the F_2 layer, and it is determined by the following formula:

$$\begin{aligned}&(dN/dh)_{\max}\left[10^9\ m^{-3}\ km^{-1}\right]\\ &= \exp\left\{-3.467 + 0.857\ln[(f_oF_2)^2] + 2.02\ln(M_{3000}F_2)\right\}.\end{aligned} \quad (23)$$

When F_2 and E layers are both present in the ionograms, the bottom-side profile is constructed as a sum of two identical Epstein layers [*Rawer*, 1988]:

$$N(h) = 4N_m \exp[(h - h_m)/B_{bot}]\{1 + \exp[(h - h_m)/B_{bot}]\}^{-2} \quad (24)$$

where N_m and h_m are the (F_2 or E) layer's peak density and peak height, respectively. The electron density distribution at D region heights is not modeled in detail.

4.3. Upper (O^+-H^+) Ion Transition Level

[25] The relative abundance of hydrogen ions is a significant factor affecting the topside electron density profile, hence the O^+-H^+ transition level can be successfully utilized as a reference point. This transition level is particularly useful because it is always above the F layer peak height and it can be determined independently (from satellite measurements). The UTL, is determined from a model [*Kutiev et al.*, 1994], based on satellite in situ measurements of the individual O^+ and H^+ ion densities. In this empirical model, the transition level is approximated by a multivariable polynomial, providing convenience when referencing the level with respect to solar activity, season, local time, longitude, and latitude:

$$P(C, N; X) = \sum_{i_1=1}^{n_1}\sum_{i_2=1}^{n_2}\sum_{i_3=1}^{n_3}\sum_{i_4=1}^{n_4}\sum_{i_5=1}^{n_5} C(i_1, i_2, \ldots i_5) \cdot g_1(i_1, x_1) g_2(i_2, x_2) \ldots g_5(i_5, x_5), \quad (25)$$

where $C = \{C(i_1, i_2, \ldots, i_5),\ i_m = 1, \ldots, n_m\}$ are the coefficients and $\{g_m(i_m, x_m)\}_{i_m=1}^{n_m}$ is a system of linearly independent functions on the domain of the mth parameter x_m, e.g., algebraic basis (1, x, x^2, …, x^{n_m}), trigonometric basis (1 sin x, cos x, …, sin $n_m x$, cos$n_m x$), etc. The method of least squares fit is applied for determining the coefficients.

5. Evaluation Results

[26] In this part, the most important ionosphere "profilers": exponential, sech-squared, and Chapman (both α and β type) are further examined as reconstruction tools [*Stankov*, 2002a]. The evaluation is performed from several aspects and important evaluation results are provided with the purpose to determine the most suitable profiler for given geophysical conditions. First, the vertical distribution is obtained with fixed O^+ scale height, peak density, and peak height. It aims at comparing the overall simulation ability of the profiler. Second, given a TEC value, fixed for given season and local time, the reconstruction is performed with each profiler and the results are estimated and compared. This task aims at determining the most suitable profiler from a reconstruction point of view. Third, using measurements from a 24-hour period, exemplary calculations have been carried out to determine the ability of reconstructing the diurnal ionosphere behavior.

5.1. Satellite In Situ Observations for Comparison Purposes

[27] Density profiles, obtained by the analytical models described in the previous section, will be compared with independent measurements. Relatively good altitude profiles of ion densities can be obtained from the Atmosphere Explorer-C (AE-C) satellite in situ measurements. The satellite was launched on 13 December 1973, in an elliptical orbit (inclination 68.1°) collecting a large database of ionospheric and thermospheric densities, temperatures, winds, and emissions within the altitude range of 130–4300 km. After the first 8 months, the mode was changed and the spacecraft was kept in a circular orbit for the rest of its lifetime (reentry date 12 December 1978): from March 1975 to December 1976 at about 300 km height, and from December 1976 to 1978 at about 400 km height.

[28] The O^+ and H^+ ion density data used here are obtained during the first 16 months of the AE-C mission, from 16 December 1973 to 21 March 1975 when the solar activity was low, F10.7 $\approx$ 85 W m^{-2} Hz^{-1}. The measurements are from both the Bennett and magnetic ion-mass spectrometers. Three seasons are considered: winter, equinox, and summer, defined as 91 day periods centered on the 356, 81 and 264, 173 days of year respectively. Daytime and nighttime conditions are investigated using data from variable local time ranges (windows) depending on the season. Larger daytime windows (0800–1700 hours) are used for summer values and larger nighttime windows (1900–0500 hours) are applied on the winter data. Middle-geomagnetic latitudes (20°–50°N) and the Northern Hemisphere will be only presented. Averaged profiles are provided in Figures 3 and 4 for both O^+ and H^+ densities.

[29] In order to test the analytical models against the actual data, some basic density profile characteristics should be extracted from the averaged data. Particularly important for the unique determination of a profile are the F_2 layer density maximum and height and also the O^+-H^+ transition level (UTL). These characteristics can be determined in the way described below and in Figure 3.

[30] The first important characteristics to extract are the density peaks and their heights for both the O^+ and electron density profiles. If quality data is available the extraction is straightforward. If not, the parabolic layer can be used to fit the data near the F_2 layer density maximum.

[31] The next important parameter to be extracted from the data is the O^+ ion scale height, H_{O^+}. The scale height is defined as the vertical distance in which the concentration changes by a factor of e ($e \approx 2.718286$). This definition allows the extraction of the scale height from the average satellite measurements. The scale height varies with height but at this stage of developing the method, it is assumed to be constant. Because of this assumption, it is important to deduce the scale height from the area immediately above h_mF_2, which contributes most to the TEC value. The curvature of the O^+ density profile does not allow the determination to begin from H_mF_2 so it starts from an altitude $h_mF_2 + h_\varepsilon$, where h_ε is approximately the half thickness of the fitting parabola. Measurement data is in abundance in this region and the scattering is generally small.

[32] The propagation factor $M_{3000}F_2$ is obtained after fitting the satellite data with Epstein layer functions. The E layer critical frequency, f_oE, is set to zero during night and the daytime values are set to some plausible values for the season and local time at the corresponding latitude. For the

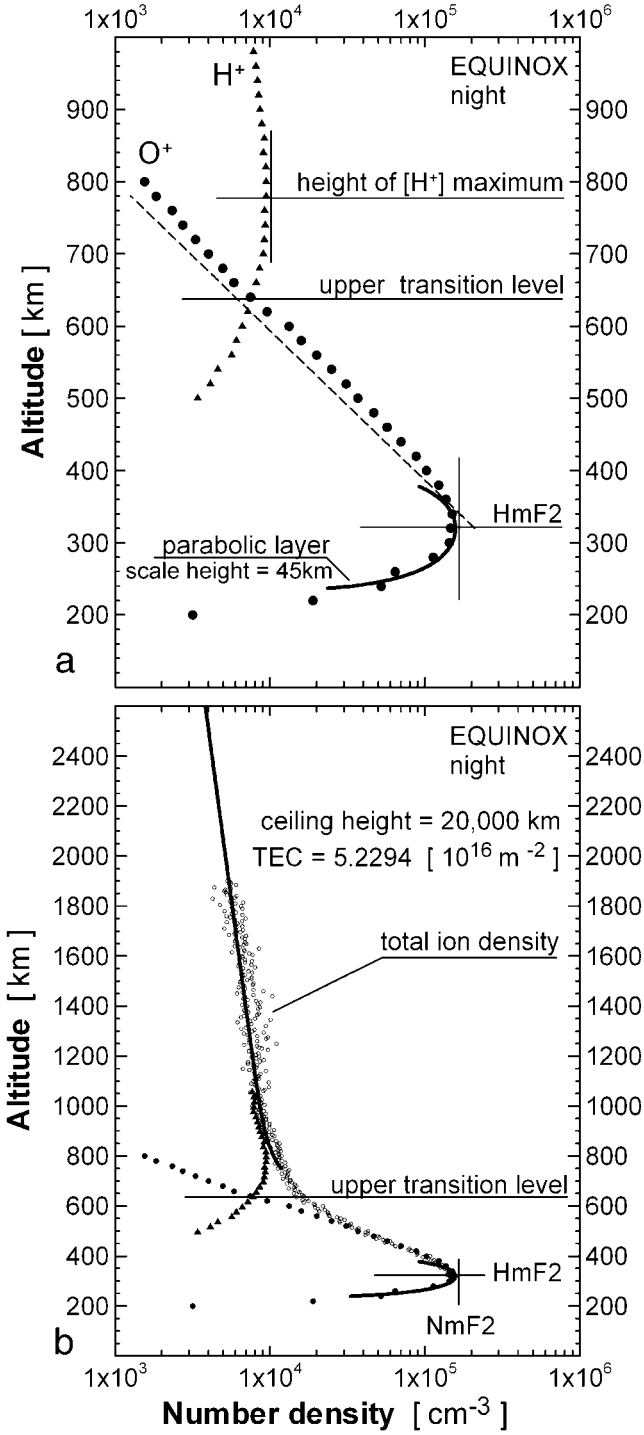

Figure 3. Basic profile characteristics deduced from satellite data: H_mF_2, N_mF_2, scale height, and upper transition level (a) and TEC value (b).

purpose of this study, the precise determination is not important as the bottom-side electron profile is fitted with the same Epstein layer that is used in the reconstruction technique.

[33] The O^+-H^+ transition height is relatively easy to determine during night when the O^+ scale height is relatively small. During daytime, the data scattering is larger because of the strong latitude dependence on latitude. In such cases, a power approximation of the oxygen ion profile near the UTL area usually helps.

[34] The last characteristic to determine is the TEC value. This is done by integrating the satellite-data-based electron density profile. In all cases, the electron profile has to be extrapolated to some large altitude. For the purpose, the hydrogen ion scale height is first deduced from the available data above the H^+ density peak and then exponential layer is employed to simulate the distribution up to the ceiling height of 20,000 km. The profile-based TEC value is calculated using quadratures [*Dahlquist and Bjorck*, 1974].

[35] Averaged altitude profiles are given in Figures 3 and 4 where the symbols represent ion density averaged over 20 km in altitude. The total ion density is given with open circles for averages over 5 km. For the case in Figure 3, TEC is found to be approximately $5.2294 \times 10^{16}[m^{-2}]$.

5.2. Electron Density Height Distributions Obtained With a Same Scale Height

[36] The vertical ion and electron density distribution produced with the same scale height of 100 km is given in Figure 2 for the four profilers: exponential, sech-squared, α-Chapman, and β-Chapman. It is obvious that the different profilers produce quite different altitude distributions in the *F* region and therefore they will produce significant differences in the corresponding values of the TEC. The largest contribution for the TEC value comes from the region near the peak height and it is most important to compare the performance mainly in this region.

[37] In order to determine which model gives better results for the O^+ density profile, all input parameters have been extracted from the averaged O^+ profiles obtained from AE-C data as described in the previous section (section 5.1). The required parameters are: the O^+ peak height (h_m), the peak density ($N_{O^+}(h_m)$), and the scale height (H_{O^+}). The retrieved parameters are listed in Table 1 for the three seasons of interest (winter, equinox, summer), and for daytime and nighttime conditions.

[38] Having obtained the key profile characteristics, the corresponding O^+ density profiles are calculated and compared again with the averaged AE-C data profiles (Figure 4). For each individual set of season and local time conditions, one scale height value was used for all four profilers. Only the sech-squared and exponential profiles are given in the figure, because the relative behavior presented in Figure 2 is preserved. It seems that the sech-squared model is more suitable for describing the nighttime behavior, while the daytime behavior is better represented by the exponential and β-Chapman models. The latter ensures better simulation in the region near the peak. The sech-squared and α-Chapman layers generally overestimate the daytime values. If the profiles are forced to pass through a given point, i.e., given density at a given height, then the shape changes as it will be seen below.

5.3. Electron Density Profile Reconstruction Obtained From a Same TEC Value

[39] It is obvious from the vertical density distribution produced with a same scale height for all profilers (Figure 2) that the largest density values at all altitudes are obtained with the α-Chapman profiler and the smallest with the exponential layer. Hence for a fixed scale height, largest

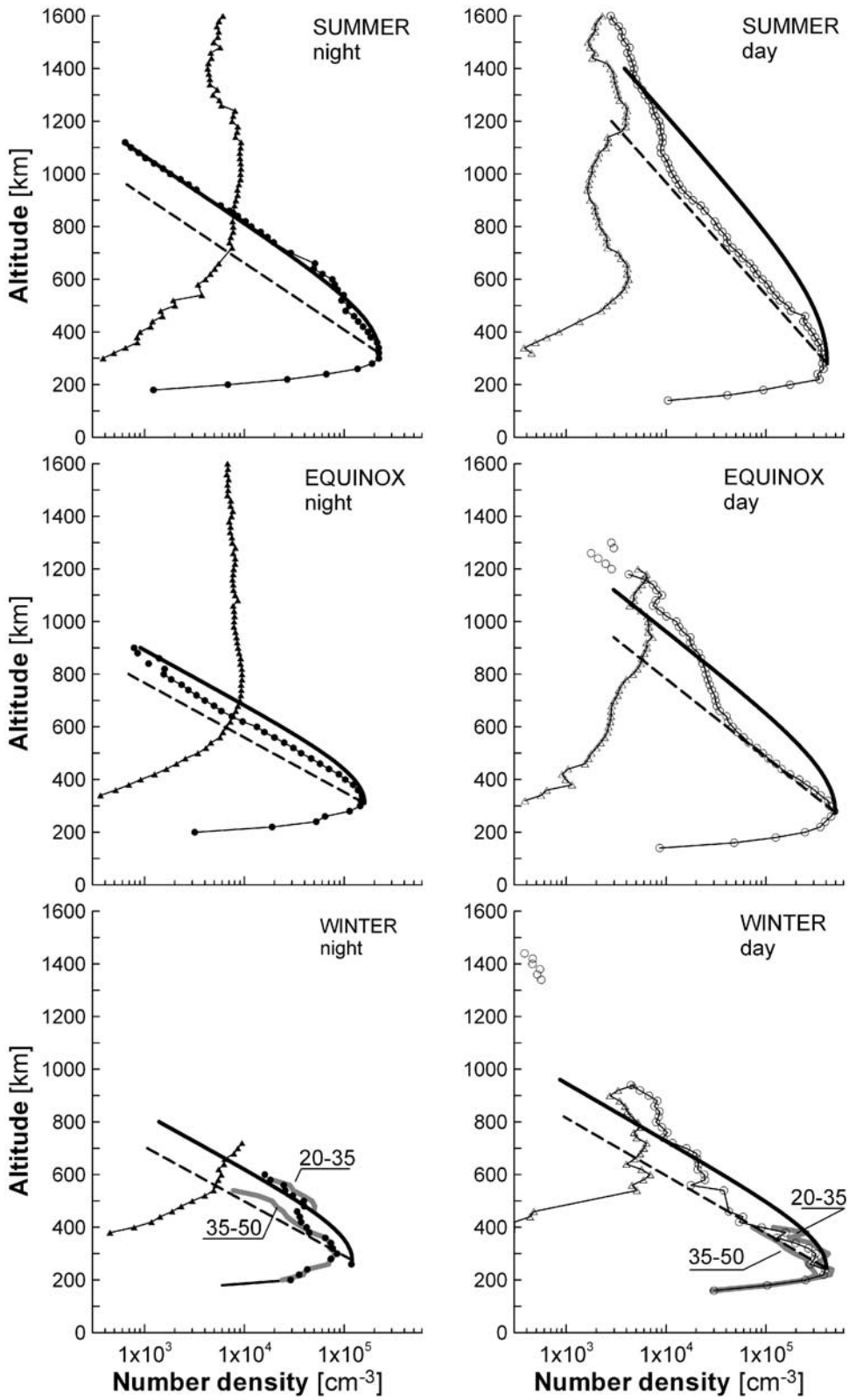

Figure 4. Sech-squared (solid line) and exponential (dashed line) O^+ profiles compared with AE-C measurements of O^+ (circles) and H^+ (triangles) densities from 20° to 50°N geomagnetic latitude range. For wintertime, the averaged profiles from 20° to 35°N and 35° to 50°N are also given.

Table 1. Basic O^+ Density Profile Characteristics Extracted From AE-C Data

Parameter	Winter	Equinox	Summer
F10.7, W m^{-2} Hz^{-1}	80.18	84.48	90.20
Dipole latitude, deg	20°–50°N	20°–50°N	20°–50°N
	Daytime		
Local time, hours	0800–1600	0800–1630	0800–1700
H_{O^+} (h_m), cm^{-3}	4.03×10^5	4.96×10^5	4.10×10^5
h_m, km	245	275	280
N_{O^+}, km	95	130	185
	Nighttime		
Local time, hours	1900–0500	2000–0430	2000–0400
N_{O^+} (h_m), cm^{-3}	1.20×10^5	1.58×10^5	3.00×10^5
h_m, km	275	320	320
H_{O^+}, km	90	90	110

TEC values are expected from the α-Chapman profiler and smallest from the exponential layer. However, in order to investigate the reconstruction quality of each profiler, it will be necessary to find out how the reconstructed profiles will look for fixed TEC and UTL values.

[40] The results in the previous section (section 5.2) suggest that in order to preserve the same TEC value, the calculated O^+ scale height using the reconstruction method should be the largest if the exponential layer is employed, and oppositely, it should be the smallest if the α-Chapman layer is used. To prove such dependence, the method was tested for a fixed UTL and fixed TEC value of 15.0×10^{16} [m^{-2}]. The results are given in Figure 5 for UTL = 1000 and 1500 km.

[41] As expected, the scale height obtained via the exponential layer is the highest: H_{O^+} = 194 km for UTL = 1000 km and H_{O^+} = 244 km for UTL = 1500 km which in result yields much steeper electron density profile. Lowest scale height values are obtained with α-Chapman: 78 and 94 km, respectively. However, because of the profiler's definitions and the different ways of simulating the density distribution near the maximum height h_m, the reconstructed Chapman-like distributions both lie in-between the "boundary" profiles obtained with the exponential and sech-squared profilers. Also, because of the differences at h_m, all reconstructed profiles intersect at a given altitude somewhere below the UTL.

[42] As a result of the differences in the calculated oxygen ion scale heights, significant differences are observed in the hydrogen ion density profiles: both in scale height and in absolute ion density values. These differences are increasing when increasing the UTL (Figure 5), which once again underlines the importance of using correct UTL values. The influence of the UTL on the scale height calculations is presented in Figure 6 for the sech-squared profiler, leading to the following conclusions [*Stankov et al.*, 2002]. First, the scale height calculations are much stronger bound to the transition level during nighttime than during daytime; a possible reason is the lack of E layer at night. An error induced

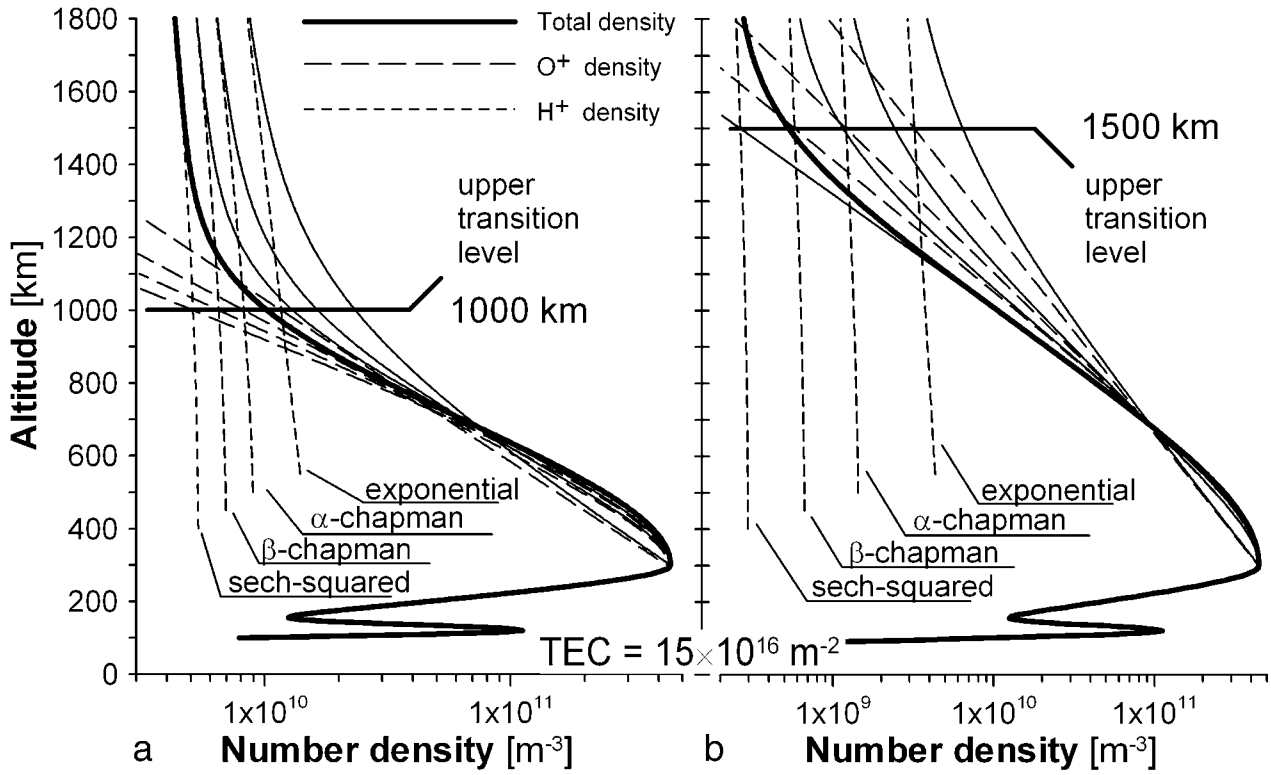

Figure 5. Comparison between the vertical ion and electron density profiles reconstructed from a same total electron content value, TEC = 15.0×10^{16}[m^{-2}], but using different upper ion transition level values: UTL = 1000 km (a) and UTL = 1500 km (b). The calculated O^+ scale heights (for UTL = 1000/1500) are: Exponential = 194/244 km, Sech-squared = 120/136 km, α-Chapman = 78/94 km, β-Chapman = 135/157 km.

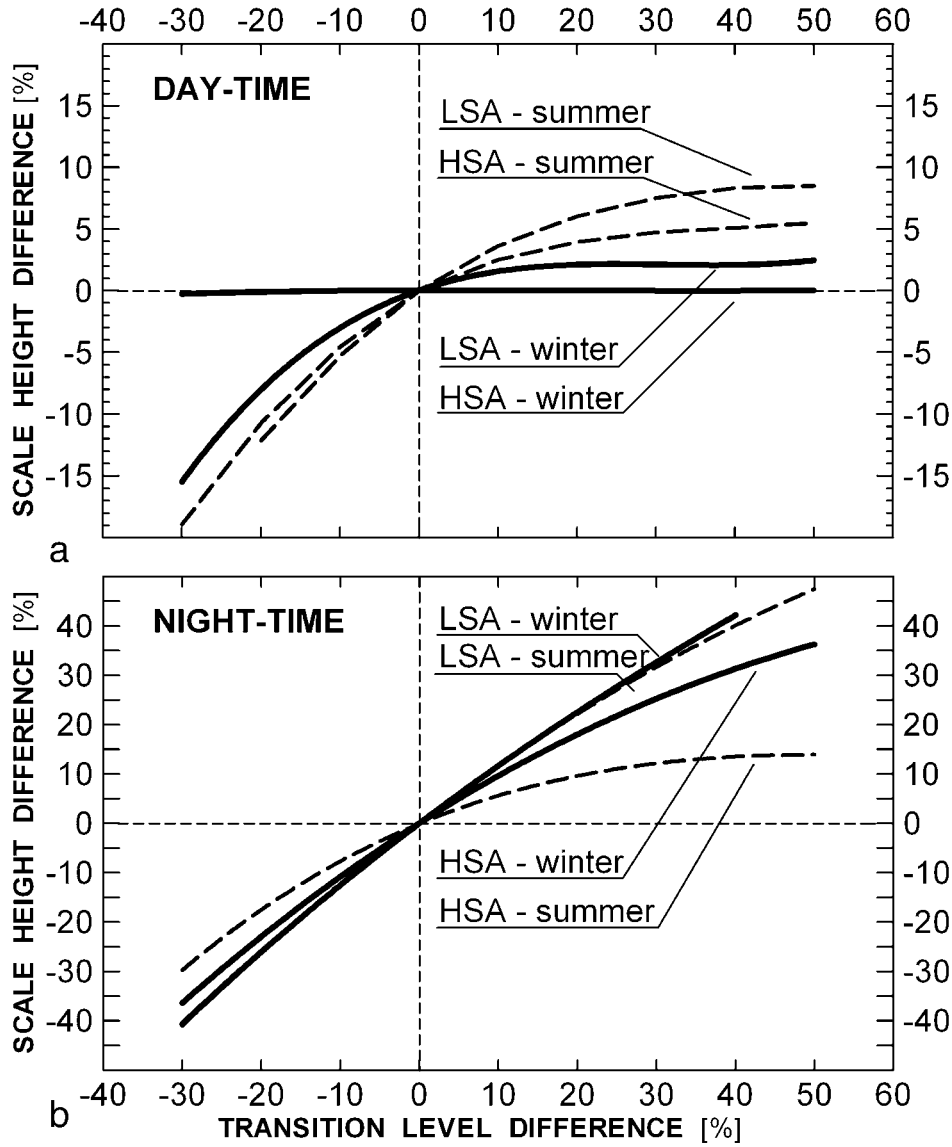

Figure 6. The oxygen ion scale height plotted as a function of the O^+-H^+ transition height for daytime (a) and nighttime (b) conditions. The vertical line represents the "perfect" transition height provided by the empirical model.

by the transition level input will lead to a larger error in determining the scale heights during night. The scale height calculation error due to overestimated transition level is expected to be not larger than 10% during daytime but higher (up to 50%) during nighttime. Second, the scale height gradient decreases when increasing the transition level. This is clearly observed during the day. The transition level cannot be increased indefinitely because at a certain level the scale height determination procedure becomes insensitive to further increase, e.g., during winters of high-solar activity. This can be explained with the very small part of TEC left to be "distributed" at altitudes above the transition level.

[43] The next step in the evaluation procedure is to deduce the density profiles using the reconstruction technique and evaluate them against averaged data profiles. The results for equinox nighttime and daytime conditions will be discussed in more detail because the available data is more reliable.

5.3.1. Nighttime Conditions

[44] All extracted profile characteristics (Table 1) are used to reconstruct the profiles for the four models under investigation. The results are presented in the four panels of Figure 7. In order to better analyze the quality of the reconstruction, the relative errors are presented in the same figure for the oxygen and electron profiles. At first glance, it is obvious that no single profile is markedly better than the others when representing the altitude density distribution. The O^+ profile is best modeled by the α-Chapman layer at lower altitudes and equally good by the β-Chapman and sech-squared profilers near the upper transition layer. The region above UTL (640 km) is not so important in the case of the O^+ profile. The situation is slightly different for the electron profile. Starting from H_mF_2, the sech-squared and

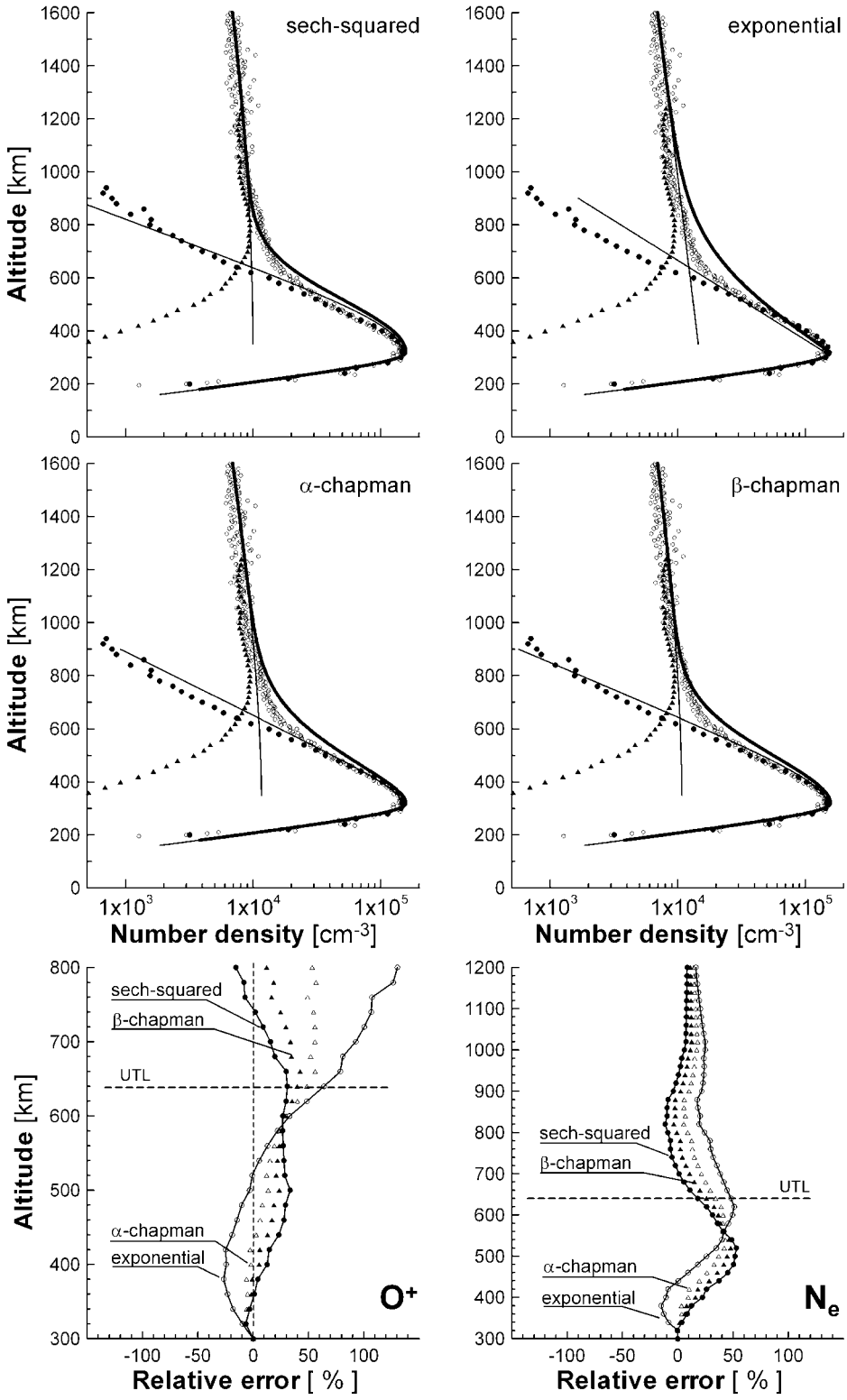

Figure 7. Nighttime ion and electron density profiles: reconstructed using sech-squared, exponential, and Chapman profilers and compared with AE-C averaged density profiles. TEC = 5.2294×10^{16} [m^{-2}], UTL = 640 km.

Chapman profilers demonstrate very good approximation up to about 400 km. From this altitude, up to the altitude of the "profile crossing" point (560 km), the exponential layer is much better than the others. For the region above, the sech-squared layer and β-Chapman are the better choices. Overall, for nighttime electron density distribution at equinox, it is best if the Chapman profiles are used, i.e., the α-type at lower altitudes and β-type for the region above the intersecting point. The calculated nighttime TEC is $5.2294 \times 10^{16}[m^{-2}]$.

5.3.2. Daytime Conditions

[45] The averaged O^+ profiles show rather large variability in the scale height. It is mainly due to the strong altitude variations in the ion temperatures during daytime. Also, the density distribution and consequently the O^+-H^+ TL vary strongly in latitude direction, so the averaged profiles reflect these facts. In order to decrease the influence of the latitude dependence, the data has been extracted from a smaller latitude band (27.5°–42.5°N). The density scattering is still high and the O^+ and H^+ profiles have been approximated. The O^+ profile has been fitted (power approximation, standard deviation = 0.045) in the height region from 640 km to UTL (1330 km). Above the H^+ profile maximum (~1020 km), the H^+ density was again extrapolated using exponential layer with scale height approximately 16 times larger than the O^+ scale height near this altitude (1020 km). The electron density profile is calculated from the fitted O^+ and H^+ densities. All reconstructed profiles are given in the top four panels of Figure 8, and the relative errors using the fitted profiles are given at the bottom of the figure. During daytime, the exponential layer is undoubtedly the best choice. It provides better overall results for the individual ion density profiles as well as for the total ion/electron density. The estimated daytime TEC value is much higher, 12.3820×10^{16} $[m^{-2}]$.

[46] For summer conditions, the best options are the sech-squared layer for nighttime and the exponential profiler for daytime conditions. During winter the data is scarce and highly scattered and it is difficult to draw decisive conclusions. However, the winter values at least prove the necessity of a more detailed look on the reconstructed patterns in latitude direction. For example, Figure 4 suggests that for winter nighttime conditions, better results are provided by the sech-squared profiler at lower latitudes and by the Chapman profiler at higher latitudes. The exponential layer is again the best option for the winter daytime conditions.

[47] Uncertainties in the evaluation procedure have been introduced via possible incorrect determination of TEC and also through the larger values of H^+ density below the H^+ peak because of the assumption for equal heights of the O^+ and H^+ density maxima. Additional studies are required for highsolar activity conditions.

5.4. Exemplary Calculations: Reconstruction of the Diurnal Behavior

[48] As an exemplary demonstration of the reconstruction technique, the electron density is reconstructed over an extended (24-hour) period of time. The example covers the diurnal behavior of the vertical electron density distribution during summer solstice at highsolar activity for station Juliusruh (ionosonde code JR055, 13.38E, 54.63N); results are plotted in Figure 9. The input values of the GPS-derived TEC, together with the vertical sounding measurements of f_oF_2, $M_{3000}F_2$, and f_oE, are given in the middle panel of Figure 9. The TEC and f_oF_2 show strongly correlated diurnal behavior. Both quantities increase sharply in the early morning, reach their absolute maximum just before noon, and then start gradually decreasing. Relatively high values are maintained throughout the afternoon, followed even by a 10% increase in the early evening. After that, both TEC and f_oF_2 fall rapidly to their corresponding absolute minima observed at 0200–0300 LT. In the bottom panel of Figure 9, the empirically modeled heights of F_2-peak-density and O^+-H^+ ion transition are also provided. The transition level, starting from 1000 km at midnight, increases up to slightly above 1400 km at noon and then decreases in a symmetrical fashion during the second half of the day. On the other hand, H_mF_2 has highest values at midnight (around 400 km) and lowest values during day (varying between 300 and 330 km). The reconstructed electron density distribution is plotted in the top panel of Figure 9. Notice the detailed vertical distribution above the H_mF_2: it is easy to detect the changes in the calculated topside scale height and the resulting density distribution as they develop during this particular 24-hour period.

6. Application: Operational Real-Time Reconstruction of the Electron Density Distribution

[49] In the section 5.4, the reconstruction was applied at a single-ionosonde location over a 24-hour period. It is generally unproblematic to extend the method to cover all ionosonde locations, thus producing maps of the electron density. Especially for the European region, it is possible to obtain two- and three-dimensional electron density distribution.

[50] Perhaps the most valuable application of the reconstruction technique is the operational reconstruction on a real-time basis. The real-time access to the top-side electron density distribution, reconstructed via the described method, widely opens the door to attacking many (old and new) problems of importance, such as the estimation and correction of the propagation delays in the GNSS, verification of empirical and theoretical ionosphere-plasmasphere models, operation of satellite augmentation systems, space weather effects on telecommunications, etc.

[51] A new operational procedure for reconstruction of the ionosphere-plasmasphere vertical electron density distribution on a real-time basis is presented below. The core of such defined operational model is the above reconstruction technique, which uses various types of concurrent observations (GPS TEC, ionosonde, direct satellite) to reliably deduce the most adequate electron density height profile at a given location and for the time of observations. Another important ingredient of the operational model is the procedure for operating the reconstruction. Apart from "managing" the reconstruction, it also takes care of collecting, transferring, and processing the measurement data in a fast and reliable way. Important issues in such "data assimilation" procedure are data digitalization, network reliability, strict time control, etc. Details are also given further below. Tests have been already executed with actual measurements obtained at the Belgian Royal Meteorological Institute's

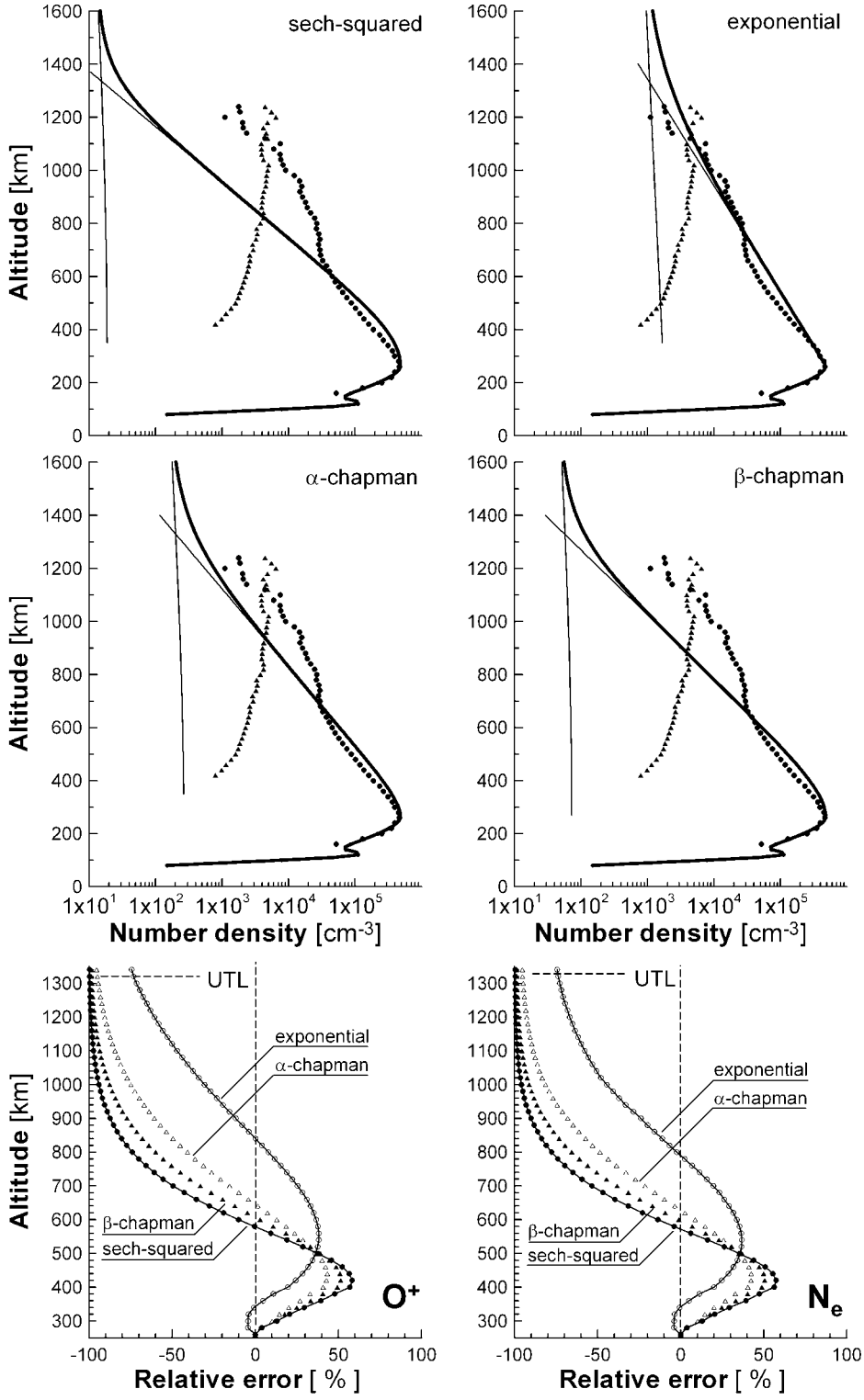

Figure 8. Daytime ion and electron density profiles: reconstructed using sech-squared, exponential, and Chapman profilers and compared with AE-C averaged density profiles. TECTONICS, VOL. = 12.3820 $\times$ 10^{16} [m^{-2}], UTL = 1330 km.

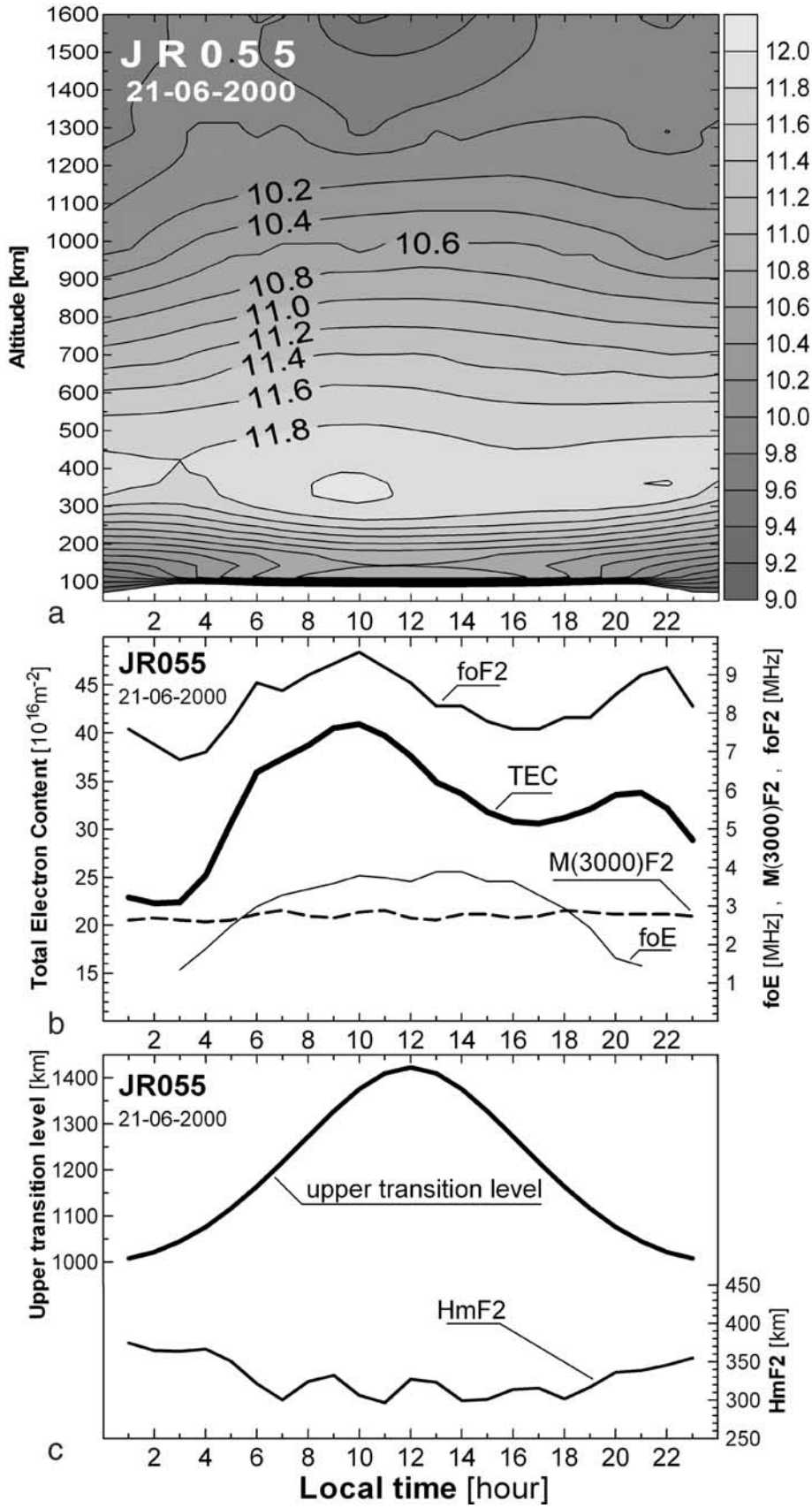

Figure 9. Diurnal ionosphere behavior reconstruction. (a) Reconstructed vertical electron density (log scale, m^{-3}). (b) GPS TEC and required ionosonde measurements. (c) Upper transition height model.

Geophysics Center at Dourbes (4.6°E, 50.1°N). Preliminary results are presented and discussed.

[52] In general, the operational procedure is a stand-by procedure: its execution is triggered by either a time control system or the arrival of new measurements. Thus it relies heavily on regular influx of ionosonde, geomagnetic, and TEC discrete measurement data. All types of observations should be synchronized and processed quickly, so that representative results can be obtained for a given location and a time. Highest flexibility, in terms of time resolution, is offered by the digital ionosonde: new measurement data are available within a delay of about 5 min. Longer delay is expected for receiving the GPS TEC value, because the TEC derivation procedure requires time and sufficient number of measurements. In practice, a TEC value can be obtained every 15 min, which is sufficient for most applications.

[53] Several distinct stages are observed in the operational reconstruction procedure: transmission of measurement data and retrieval of input parameters, construction of the bottom and topside electron profile, backup and display of results. The data are transmitted using the File Transfer Protocol; the UTL values are provided by an empirical model incorporated into the reconstruction software. If the TEC value is not available on time, it is possible to use the ionosonde-based TEC value; the mean and standard deviations for low-solar activity (LSA) are estimated at approximately 0.46 and 1.72 TECU. Analytical expressions are also available for h_mF_2. For the retrieval of the topside electron profile, it is necessary to adopt a theoretical ''profiler'' for the topside oxygen and hydrogen ion densities; in our case the sech-squared and exponential layers are chosen. In the final stage of the procedure, all results are stored and displayed. Thus the system is ready for the next round of calculations.

[54] The new operational model, based on the presented procedure and reconstruction method, has been tested with actual hourly values of GPS TEC and ionosonde measurements acquired in real-time mode at the RMI Geophysics Center. A trial run started at 0000 LT on 11 March 2002, and finished at 2400 LT on 17 March 2002. During this period, the solar activity was relatively high ($176 < F10.7 < 185$) and geomagnetic activity conditions were quiet ($Ap < 12$). Reconstructed electron profiles were ready for display well before the 15-min time delay limit. Therefore the operational model is capable of producing profiles every 15 min using new observations, which is a sufficiently good rate for most of the envisaged applications (storm investigation included). Considering the evaluation results from section 5, the sech-squared layer was applied for nighttime conditions only, while the exponential profiler was used for the daytime hours, 0700–1900 LT. The results of this run are provided for the period 11–13 March 2002 (Figure 10). The reconstructed topside electron concentration is highly sensitive to the changes in the input parameters. For example, the sharp increase in the f_oF_2 value near 0600 LT on 11 March 2002, results in a sharp decrease in the slab thickness and depleted electron density above H_mF_2. Local measurements of the geomagnetic field's horizontal component (H), delivered in real time, are important for the operational reconstruction procedure. The Dst and Kp are not available operationally, so H can be used as a substitute online indicator of geomagnetic storm activity. However, further investigations are required on the proper utilization of this input parameter.

7. Application: Reconstruction of the Electron Density Distribution From Over-Satellite Electron Content Measurements

[55] The method was originally developed for ground-based measurements of the GPS TEC. However, the flexibility of the approach permits the use of space-based GPS TEC measurements instead. Recent developments in the satellite technology allow the signal receiver to be placed onboard a LEO satellite, therefore measuring the so-called over-satellite electron content (OSEC), i.e., the integral of the electron density from the height of the receiving LEO satellite up to the ceiling height of the GPS satellite (Appendix E). Vertical incidence sounding and UTL data are still required for the reconstruction purposes. The method has been tested with GPS TEC measurements from the German LEO satellite CHAMP, which has been launched on 15 July 2000, into a circular and polar orbit (inclination = 87°) at an initial altitude of 454 km [*Reigber et al.*, 2000]. Some exemplary calculations are given in Figure 11 for both nighttime and daytime conditions.

8. Conclusions

[56] The reconstruction of the electron density height profile from TEC measurements, using UTL and ionosonde data, is a new technique utilizing different types of measurements to solve a long-lasting ionospheric physics problem. The method employs new formulae based on Chapman, sech-squared, and exponential ionosphere profilers to construct a system of equations, the solution of which system provides the unknown ion scale heights, sufficient to construct a unique electron density profile at the site of measurements. A particular attention is drawn the calculation of the scale height in the upper ionosphere, from the F_2 layer density peak height up to the O^+-H^+ transition level. In this upper ionosphere region with comparatively large contribution to the TEC value, O^+ is the major ion. Hence the O^+ ion scale height is the most important unknown parameter and it should be determined in the most precise way. All formulae are based on the assumption of diffusive equilibrium with constant scale height for each ion species

[57] Several conclusions can be deduced:

[58] 1. The importance of the reconstruction technique should be considered from the following aspects: reliability, flexibility, and applicability. The reliability of the approach is based on the routine measurements of over-satellite TEC and ground-based ionosonde soundings. Also, the reconstruction procedure employs established, efficient, and fast numerical methods. The approach provides flexibility in terms of structuring, upgrading, and testing: choice from various topside profilers, possibility of incorporating the helium ion density in the above equations, convenience when testing the method with different types of measurement data, etc. Recent advances in the regular space monitoring utilizing GNSS signals offer opportunities to apply the proposed reconstruction technique for both devel-

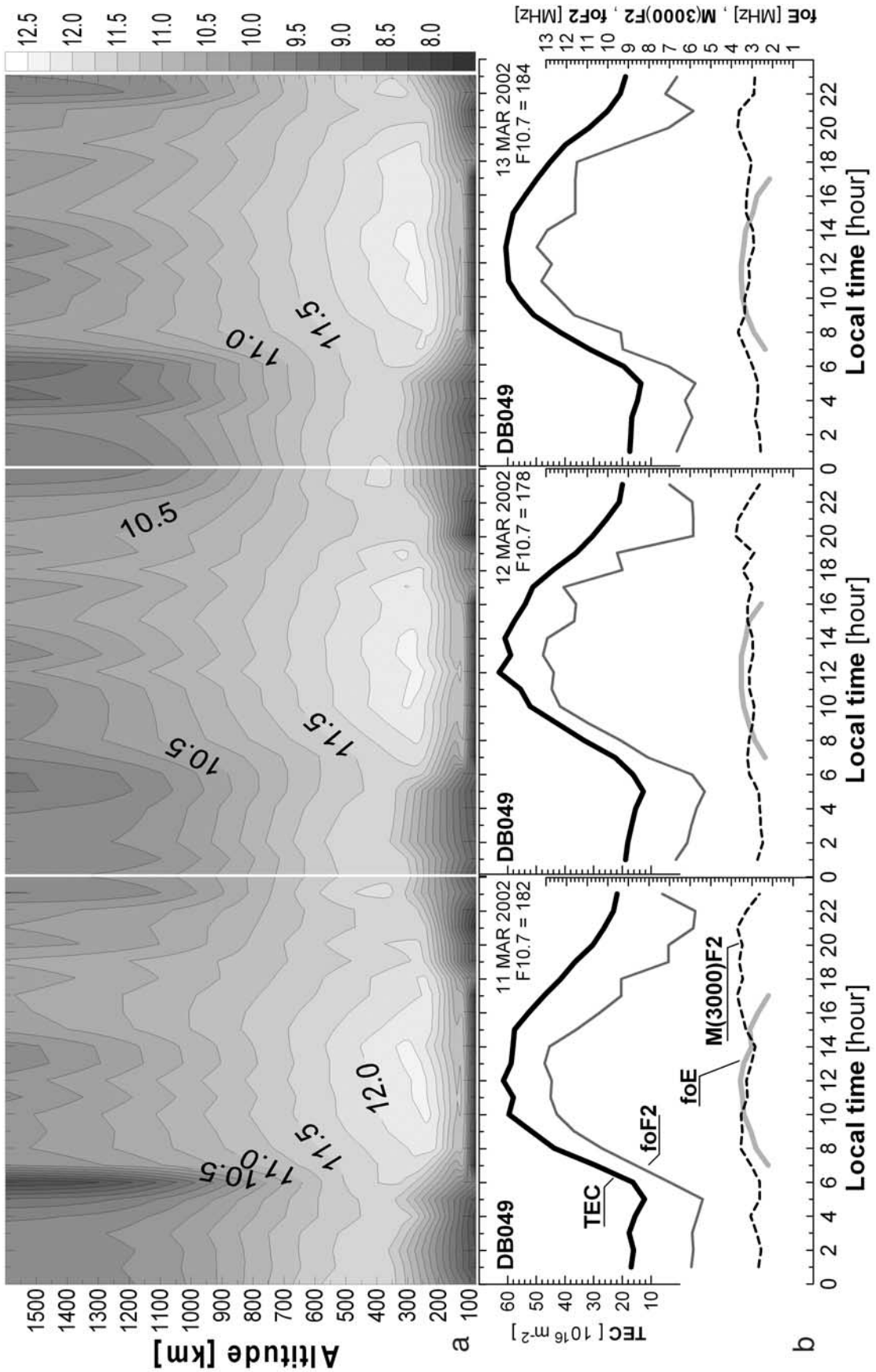

Figure 10. Real-time reconstruction of the vertical electron density distribution, 11–13 March 2002, Dourbes (4.6°E, 50.1°N). (a) Reconstructed vertical electron density (log scale, m^{-3}). (b) GPS TEC and required ionosonde measurements.

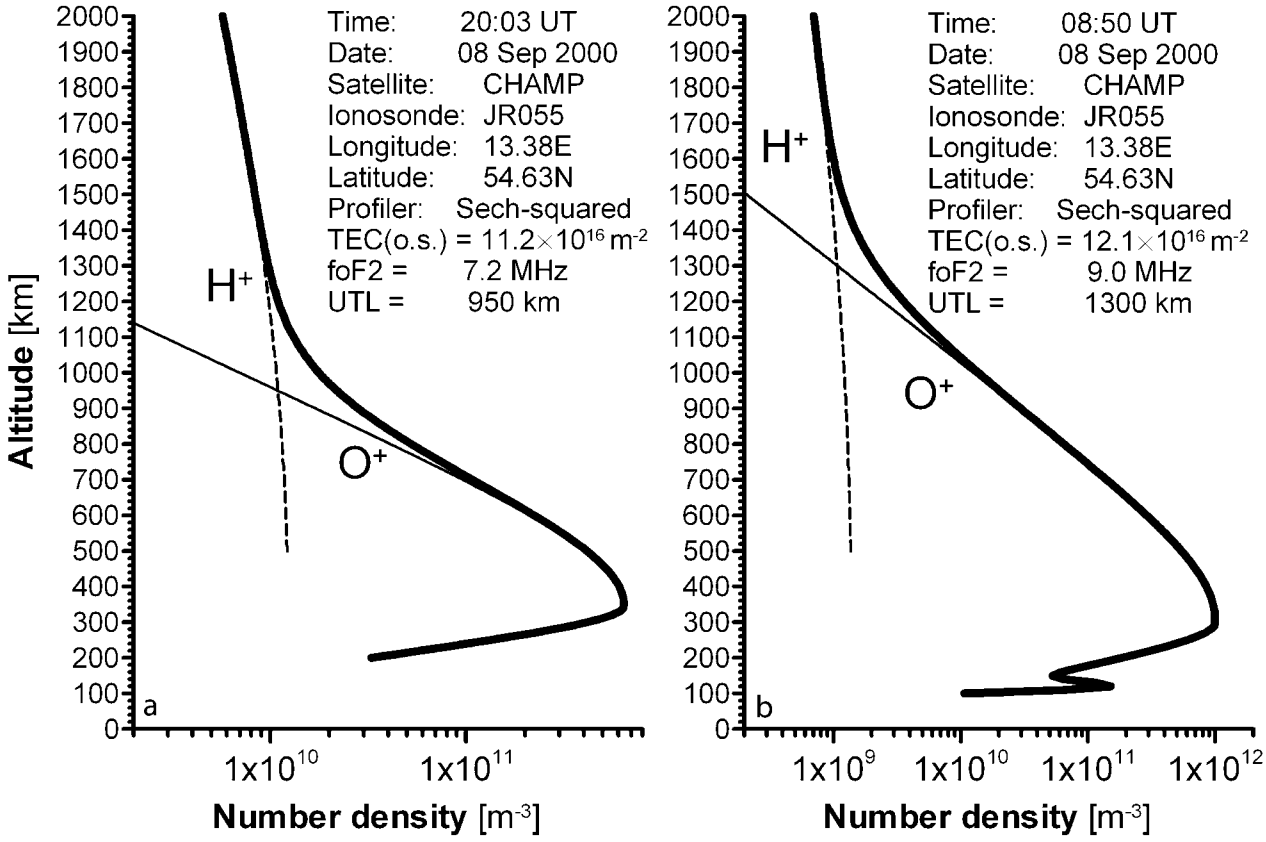

Figure 11. Reconstructed O^+, H^+, and total ion densities using CHAMP-based over-satellite electron content measurements for nighttime (a) and daytime (b) conditions.

oping and evaluating various empirical and theoretical models of the ionosphere-plasmasphere system.

[59] 2. The performance of the most widely used analytical ionospheric models (Chapman, sech-squared, and exponential) has been evaluated as they are important ingredients in the method of reconstructing the topside ion/electron density profiles. Although the density profiles produced by the sech-squared and Chapman models differ from the exponential layer profiles at lower altitudes, they tend to asymptotically approach the exponential layer distribution at great altitudes. All profilers can be successfully used in the reconstruction technique. However, no single profiler can sufficiently well represent the entire spectrum of spatial and temporal variations. For example, the parabolic layer is not suitable for reconstruction but is a very helpful tool for simulation and extraction of profile characteristics near the density maxima. Also, for daytime conditions, the exponential layer is more suitable than the other profilers for modeling/reconstruction purposes, while for nighttime conditions, the sech-squared and Chapman models guarantee better results. Moreover, it became evident that in different altitude ranges some profilers yield better results than the others. The latter implies that a composite profiler/profile should be developed in order to obtain generally better results (a typical example of a composite profile is the IRI height distribution). However, the problem is complicated, as it requires further mathematical calculations and larger GPS-TEC database. For example, data are still not available for a full solar activity cycle.

[60] 3. The UTL plays a key role in the reconstruction procedure. One of the main ideas behind the reconstruction technique is the use of the O^+-H^+ transition level, which not only provides for the uniqueness of the solution, but also is diminishing the eventual error introduced by the assumptions of constant scale height and diffusive equilibrium conditions. Inaccurate values of the transition level, especially during daytime, may produce significant errors in the determination of the topside O^+ and H^+ scale height (i.e., density distribution) mainly due to the high sensitivity of TEC from the slope of the electron profile which is immediately above the peak height H_mF_2. There is a pronounced need for a high-quality ionosphere-plasmasphere temperature model, which will help in determining the topside scale heights much more precisely.

[61] 4. At this stage, the offered reconstruction technique is more suitable for use at middle and high latitudes because the dipole coordinates are useful at these latitudes but can be misleading at lower latitudes where the tilt of the geomagnetic field lines (dip) is of major importance.

[62] 5. The electron density reconstruction technique proved to be very useful in developing a new procedure that would allow obtaining more information on the topside electron density distribution in a real-time mode. The developed operational procedure is reliable, easy to maintain, and upgrade. It is important that the high resolution in the input rate (on average, 10–15 min) delivers an opportunity for investigating the local ionosphere development even under storm-time conditions. However, for better

identifying and observing a storm, it is necessary to include geomagnetic field measurements, i.e., the horizontal component, in particular.

[63] In summary, the presented reconstruction technique has the potential of a powerful research instrument and can be further improved when more measurements are available from various sources. Important applications of the operational reconstruction model are envisaged, such as test and development of ionosphere-plasmasphere models, optimization of HF radio systems operation, investigation of ionospheric storms, and other space-weather studies.

Appendix A: Plasma Diffusion and Diffusive Equilibrium

[64] In the plasmasphere the neutral densities are so small that they have little effect on the charged particle motions determined by electric and magnetic fields. There is essentially no ion production; the ionization is produced in the ionosphere during the day and diffuses upward. During nighttime when the ionospheric plasma densities decrease, plasma diffuses down from the plasmasphere into the ionosphere. In both cases, the diffusion occurs along the geomagnetic field lines because diffusion across the magnetic field is inhibited. Also, because the diffusion coefficient is inversely proportional to neutral density, diffusion increases rapidly with increase of altitude. When the ions and electrons diffuse together, the process is called ambipolar diffusion.

[65] There are three basic diffusive states for plasma in the upper ionosphere: diffusive equilibrium, inward diffusion, and outward diffusion. The diffusive equilibrium is defined as the static distribution of plasma when there is no net ionization along the tubes of magnetic force, except for a small inward flow at low altitudes accommodating ion losses in the ionospheric F region. The inward diffusion occurs when the excess of plasma pressure at high altitudes drives the plasma down (inward) resulting in a net downward transport of light ions enhancing the ion density in the F region. The flow can be either supersonic or subsonic, and there are evidences that the density profiles maintained by the subsonic diffusive flow are essentially the same as those for the diffusive equilibrium. In the situation of outward diffusion, the plasma pressure gradients and the gravitationally induced electric fields, parallel to the magnetic field lines, push the light ions upward. Such flows are typical during the "recovery" phase of the ionospheric storm and ultimately the upward flowing plasma fills the field tube along which the plasma moves toward diffusive equilibrium [*Banks and Kockarts*, 1973; *Davies*, 1990].

[66] When a multicomponent plasma is placed in a gravitational field, a parallel electric field, $\mathbf{eE}_{\|}$, is established which arranges the ions in height so that lighter ions are in regions of weaker gravity. Thus in diffusive equilibrium, layers of ions are formed in inverse order of their atomic masses. Diffusive equilibrium should be expected to prevail at altitudes above the F_2 density peak, and it should extend up through the protonosphere since the ions there have an isotropic Maxwellian velocity distribution. At higher levels, the diffusion problem becomes complicated due to the presence of more than one species. The diffusive equilibrium theory was first described by *Dungey* [1955] for two ion species and for multiconstituent plasma by *Angerami and Thomas* [1964]. Also, the dynamical nature of the topside ionosphere and plasmasphere is quite complex owing to the relatively large time constants associated with the plasma flow characteristics and the frequent occurrences of plasma disturbances caused by various sources. Therefore the diffusive equilibrium appears to be difficult to reach but it provides useful theoretical foundation for investigating the dynamical plasma properties.

Appendix B: Calculation of the Topside Electron Content Using the Sech-Squared Profiler

[67] In section 3, new reconstruction formulae have been deduced using the exponential, sech-squared, and Chapman layers. An essential part in deducing the formulae is the solution of the integrals giving the topside electron content. The sech-squared (Epstein) layer is used in the following form:

$$N_i(h) = N_i(h_m)\mathrm{sech}^2\left(\frac{h-h_m}{2H_i}\right). \tag{B1}$$

The integrals in formula (7) are solved by applying the following three successive substitutions:

$$x = \left(\frac{h-h_m}{2H}\right); \quad \lim_{h\to h_{cx}} = \frac{h_c-h_m}{2H}, \lim_{h\to h_m} x = 0, \tag{B2}$$

$$y = 2x; \quad \lim_{x\to x_c} y = \frac{h_c-h_m}{H}, \quad \lim_{x\to x_m} y = 0, \tag{B3}$$

$$z = \exp(y); \quad \lim_{y\to y_c} z = \exp\left(\frac{h_c-h_m}{H}\right), \quad \lim_{y\to y_m} z = 1. \tag{B4}$$

Thus each integral is solved in the following manner:

$$\int_{hm}^{hc} N(h)dh = HN_m \int_{xm}^{xc} \frac{4e^{2x}}{(1+e^{2x})^2}dx$$

$$= 4HN_m \int_{ym}^{yc} \frac{e^y}{(1+e^y)^2}dy = 4HN_m \int_{zm}^{zc} \frac{1}{(1+z)^2}dz = 2HN_m, \tag{B5}$$

for $h_c \gg h_m$, and the topside electron content becomes:

$$\Phi_t = 2H_{O^+}N_{O^+}(h_m) + 2H_{H^+}N_{H^+}(h_m). \tag{B6}$$

Appendix C: Calculation of the Topside Electron Content Using the Exponential Profiler

[68] In section 3, new reconstruction formulae have been deduced using the exponential, sech-squared, and Chapman layers. An essential part in deducing the formulae is the

solution of the integrals giving the topside electron content. The exponential layer is defined as:

$$N_i(h) = N_i(h_m)\exp\left(-\frac{h-h_m}{H_i}\right), \tag{C1}$$

where $N_i(h)$ is the density at height h, H_i (positive) is the ion scale height. To solve the integrals in formula (7) the following substitution is applied:

$$x = \left(-\frac{h-h_m}{H}\right); \lim_{h\to h_c} x = -\infty, \lim_{h\to h_m} x = 0 \tag{C2}$$

leading to

$$\int_{hm}^{hc} N(h)dh = -HN_m \int_{xm}^{xc} \exp(x)dx = HN_m. \tag{C3}$$

Hence the topside electron content is

$$\Phi_t = H_{O_+}N_{O_+}(h_m) + H_{H_+}N_{H_+}(h_m) \tag{C4}$$

Appendix D: Calculation of the Topside Electron Content Using the Chapman Profiler

[69] In section 3, new reconstruction formulae have been deduced using the exponential, sech-squared, and Chapman layers. An essential part in deducing the formulae is the solution of the integrals giving the topside electron content.

[70] For the α-Chapman layer, the density at a given height is

$$N(h) = N(h_m)\exp\left\{\frac{1}{2}\left[1-\frac{h-h_m}{H}-\exp\left(-\frac{h-h_m}{H}\right)\right]\right\}. \tag{D1}$$

Applying the substitutions

$$x = \left(\frac{h-h_m}{H}\right); \quad x_c = \lim_{h\to h_c} x = \frac{h_c-h_m}{H}, \quad x_m = \lim_{h\to h_m} x = 0, \tag{D2}$$

$$y = \frac{1}{\sqrt{2}}\exp\left(-\frac{x}{2}\right); \quad y_c = \lim_{x\to x_c} y = \exp\frac{1}{2}\left(-\frac{h_c-h_m}{2H}\right), \quad y_m = \lim_{x\to x_m} y = \frac{1}{\sqrt{2}}, \tag{D3}$$

the integration of the α-Chapman function yields the following sequence:

$$\begin{aligned}\int_{hm}^{hc} N(h)dh &= HN_m \int_{xm}^{xc} \exp\left[\frac{1}{2}-\frac{1}{2}x-\frac{1}{2}\exp(-x)\right]dx \\ &= HN_m \int_{ym}^{yc} \exp\left[\frac{1}{2}+\frac{1}{2}\ln(2)+\ln(y)-y^2\right]\left(-\frac{2}{y}\right)dy \\ &= -2HN_m\sqrt{2e}\int_{ym}^{yc}\exp\left(-y^2\right)dy \\ &= HN_m\sqrt{2e\pi}\frac{2}{\sqrt{\pi}}\int_{yc}^{ym}\exp\left(-y^2\right)dy \\ &= HN_m\sqrt{2e\pi}\,\mathrm{erf}\left(\frac{\sqrt{2}}{2}\right) \approx 2.821HN_m\end{aligned} \tag{D4}$$

because $y_c = 0$ for very large ceiling height, $(h_c - h_m) > 20H$. Therefore the topside electron content is

$$\Phi_t = 2.821H_{O^+}N_{O^+}(h_m) + 2.821H_{H^+}N_{H^+}(h_m). \tag{D5}$$

Similarly, for the β-Chapman layer the density at a given height is

$$N(h) = N(h_m)\exp\left\{\left[1-\frac{h-h_m}{H}-\exp\left(-\frac{h-h_m}{H}\right)\right]\right\}. \tag{D6}$$

The substitutions are now

$$x = \left(\frac{h-h_m}{H}\right); \quad x_c = \lim_{h\to h_c} x = \frac{h_c-h_m}{H}, \; x_m = \lim_{h\to h_m} x = 0, \tag{D7}$$

$$y = \exp(-x); \quad y_c = \lim_{x\to x_c} y = \exp\left(-\frac{h_c-h_m}{H}\right), \quad y_m = \lim_{x\to x_m} y = 1, \tag{D8}$$

and the integration is as follows:

$$\begin{aligned}\int_{hm}^{hc} N(h)dh &= HN_m \int_{xm}^{xc} \exp[1-x-\exp(-x)]dx \\ &= HN_m \int_{ym}^{yc} \exp[1+\ln(y)-y]\left(-\frac{1}{y}\right)dy \\ &= -HN_m \int_{ym}^{yc} \exp(1-y)dy \\ &= HN_m\{\exp(1-y)\}\Big|_{ym}^{yc} = HN_m(e-1) \approx 1.718HN_m\end{aligned} \tag{D9}$$

because $y_c = 0$ for very large values of h_c, $(h_c - h_m) > 10H$ Then, the topside electron content is

$$\Phi_t = 1.718H_{O^+}N_{O^+}(h_m) + 1.718H_{H^+}N_{H^+}(h_m). \tag{D10}$$

Appendix E: The Reconstruction Technique Based on Over-Satellite Electron Content Measurements

[71] Recent advances in the GPS receiver and satellite technology allow the signal receiver to be placed onboard a low earth-orbiting (LEO) satellite, therefore measuring the over-satellite electron content, i.e., the integral of the electron density from the height of the receiving satellite, h_s ($h_s > h_mF_2$), up to the ceiling height, h_c ($h_c \gg h_s$). The ground-measured TEC, i.e $\Phi(h_g, h_c)$, is denoted $g\Phi$, while the ''over-satellite'' electron content, $\Phi(h_s, h_c)$, is denoted $s\Phi$. The over-satellite electron content, is the difference between the topside electron content (above h_m) and the

electron content enclosed between the heights h_m and h_s, i.e.,

$$s\Phi = \Phi(h_s;h_c) = \Phi(h_m;h_c) - \Phi(h_m;h_s) = \int_{hm}^{hc} N_e(h)dh - \int_{hm}^{hs} N_e(h)dh$$

Both integrals are solved similarly and the result for the sech-squared profiler is

$$\int_{hm}^{hs} N(h)dh = 2HN(h_m)\frac{1-\exp\left(\frac{h_m-h_s}{H}\right)}{1+\exp\left(\frac{h_m-h_s}{H}\right)} \quad \text{and}$$

$$\int_{hm}^{hc} N(h)dh = 2HN(h_m).$$

Further, after integrating $N_e(h)$ using the Epstein "reconstruction" formula, considering the above integral solutions, and after a series of transformations [*Stankov*, 2002b], the following transcendental equation is constructed for obtaining the unknown O^+ scale height:

$$\frac{s\Phi - 64kY_{H^+}H_{O^+}N_m}{4(Y_{O^+} - 16kY_{H^+})H_{O^+}N_m}\left\{\operatorname{sech}^2\left(\frac{h_{tr}-h_m}{2H_{O^+}}\right) + \operatorname{sech}^2\left(\frac{h_{tr}-h_m}{32kH_{O^+}}\right)\right\} = \operatorname{sech}^2\left(\frac{h_{tr}-h_m}{32kH_{O^+}}\right),$$

where k is the vertical scale height corrector (see section 2) and

$$Y_{O^+} = \exp\left(\frac{h_m-h_s}{H_{O^+}}\right)\Big/\left[1+\exp\left(\frac{h_m-h_s}{H_{O^+}}\right)\right],$$

$$Y_{H^+} = \exp\left(\frac{h_m-h_s}{16kH_{O^+}}\right)\Big/\left[1+\exp\left(\frac{h_m-h_s}{16kH_{O^+}}\right)\right].$$

Required ionosonde data again are the F_2 layer critical frequency (f_oF_2), the propagation factor $M_{3000}F_2$, and the E layer critical frequency (f_oE).

[72] **Acknowledgments.** This research has been financially supported by the German Aerospace Center, the Belgian Federal Office for Scientific, Technical, and Cultural Affairs, the Royal Meteorological Institute of Belgium, and by the NATO Science Program under grant EST.CLG.977103. The authors thank the GeoForschungs Zentrum in Potsdam for the high-quality GPS TEC data acquisition and processing.

[73] Shadia Rifai Habbal thanks Reinhart Leitinger and another referee for their assistance in evaluating this paper.

References

Angerami, J. J., and J. O. Thomas, Studies of planetary atmospheres: 1. The distribution of electrons and ions in the earth's exosphere, *J. Geophys. Res.*, *69*, 4537–4560, 1964.

Austen, J. R., S. J. Franke, and C. H. Liu, Ionospheric imaging using computerized tomography, *Radio Sci.*, *23*, 299–307, 1988.

Banks, P. M., and G. Kockarts, *Aeronomy*, Academic, San Diego, Calif., 1973.

Booker, H. G., A theory of scattering of nonisotropic irregularities with application to radar reflection from the aurora, *J. Atmos. Terr. Phys.*, *8*, 204–221, 1956.

Bowles, K. L., Observation of vertical incidence scatter from the ionosphere at 41 Mc/s, *Phys. Rev. Lett.*, *1*, 454, 1958.

Bilitza, D., K. Rawer, L. Bossy, and T. Gulyaeva, International reference ionosphere—Past, present and future, part II, Plasma temperatures, ion composition and ion drift, *Adv. Space Res.*, *13*(3), 15–23, 1993.

Chapman, S., Geomagnetic nomenclature, *J. Geophys. Res.*, *68*, 1174, 1963.

Dahlquist, G., and A. Bjorck, *Numerical Methods*, Prentice-Hall, Old Tappan, N.J., 1974.

Davies, K., *Ionospheric Radio*, Peter Peregrinus, London, 1990.

Davies, K., Ionosphere models, in *The Upper Atmosphere—Data Analysis and Interpretation*, edited by W. Dieminger, G. K. Hartmann, and R. Leitinger, pp. 693–705, Springer-Verlag, New York, 1996.

Davies, K., and G. K. Hartmann, Studying the ionosphere with the global positioning system, *Radio Sci.*, *84*, 1695–1703, 1997.

Di Giovanni, G., and S. M. Radicella, An analytical model of the electron density profile in the ionosphere, *Adv. Space Res.*, *10*, (11)27–(11)30, 1990.

Dudeney, J. R., The accuracy of simple methods for determining the height of the maximum electron concentration of the F_2-layer from scaled ionospheric characteristics, *J. Atmos. Terr. Phys.*, *45*, 629–640, 1983.

Dungey, J. W., *The Physics of the Ionosphere*, Phys. Soc., London, 1955.

Farley, D. T., Incoherent scatter radar probing, in *Modern Ionospheric Science*, edited by H. Kohl, R. Rüster, and K. Schlegel, pp. 415–439, Eur. Geophys. Soc., Katlenburg-Lindau, 1996.

Franklin, C. A., and M. A. Maclean, The design of swept-frequency topside sounders, *Proc. IEEE*, *57*, 897–929, 1969.

Gordon, W. E., Incoherent scatter of radio waves by free electrons with applications to space exploration by radar, *Proc. IRE*, *46*, 1824, 1958.

Greenwald, R. A., The role of coherent radars in ionospheric and magnetospheric research, in *Modern Ionospheric Science*, edited by H. Kohl, R. Rüster, and K. Schlegel, pp. 391–414, Eur. Geophys. Soc., Katlenburg-Lindau, 1996.

Hargreaves, J. K., *The Solar-Terrestrial Environment*, Cambridge Univ. Press, New York, 1992.

Jakowski, N., TEC monitoring by using satellite positioning systems, in *Modern Ionospheric Science*, edited by H. Kohl, R. Rüster, and K. Schlegel, pp. 371–390, Eur. Geophys. Soc., Katlenburg-Lindau, 1996.

Jakowski, N., E. Sardon, E. Engler, A. Jungstand, and D. Klaehn, Relationships between GPS-signal propagation errors and EISCAT observations, *Ann. Geophys.*, *14*, 1429–1436, 1996.

Kutiev, I., S. M. Stankov, and P. Marinov, Analytical expression of O^+-H^+ transition surface for use in IRI, *Adv. Space Res.*, *14*, 135–138, 1994.

Leitinger, R., Ionospheric electron content, in *The Upper Atmosphere—Data Analysis and Interpretation*, edited by W. Dieminger, G. K. Hartmann, and R. Leitinger, pp. 660–672, Springer-Verlag, New York, 1996a.

Leitinger, R., Tomography, in *Modern Ionospheric Science*, edited by H. Kohl, R. Rüster, and K. Schlegel, pp. 346–370, Eur. Geophys. Soc., Katlenburg-Lindau, 1996b.

Pfaff, R. F., In-situ measurement techniques for ionospheric research, in *Modern Ionospheric Science*, edited by H. Kohl, R. Rüster, and K. Schlegel, pp. 459–551, Eur. Geophys. Soc., Katlenburg-Lindau, 1996.

Phinney, R. A., and D. L. Anderson, On the radio occultation method for studying planetary atmospheres, *J. Geophys. Res.*, *73*, 1819–1827, 1973.

Rawer, K., Synthesis of ionospheric electron density profiles with Epstein functions, *Adv. Space Res.*, *8*, 191–198, 1988.

Reigber, Ch., H. Lühr, and P. Schwintzer, CHAMP mission status and perspectives, *EOS Trans. AGU*, *81*(48), Fall Meet. Suppl. Abstract 307, 2000.

Reinisch, B. W., Ionosonde, in *The Upper Atmosphere—Data Analysis and Interpretation*, edited by W. Dieminger, G. K. Hartmann, and R. Leitinger, pp. 370–381, Springer-Verlag, New York, 1996a.

Reinisch, B. W., Modern ionosondes, in *Modern Ionospheric Science*, edited by H. Kohl, R. Rüster, and K. Schlegel, pp. 440–458, Eur. Geophys. Soc., Katlenburg-Lindau, 1996b.

Reinisch, B. W., D. M. Haines, R. F. Benson, J. L. Green, G. S. Sales, and W. W. L. Taylor, Radio sounding in space: Magnetosphere and topside ionosphere, *J. Atmos. Sol. Terr. Phys.*, *63*, 87–98, 2001.

Sardon, E., A. Rius, and N. Zarraoa, Estimation of the transmitter and receiver differential biases on the ionospheric total electron content from global positioning system observations, *Radio Sci.*, *29*, 577–586, 1994.

Stankov, S. M., Evaluation of analytical ionospheric models used in electron density profile reconstruction, *Acta Geod. Geophys. Hung.*, *37*, 385–401, 2002a.

Stankov, S. M., Reconstruction of the upper electron density profile from the over-satellite electron content, *C. R. Acad. Bulg. Sci.*, *55*, 31–36, 2002b.

Stankov, S. M., and P. Y. Muhtarov, Reconstruction of the electron density profile from the total electron content using upper transition level and vertical incidence sounding measurements, *C. R. Acad. Bulg. Sci.*, *54*, 45–48, 2001.

Stankov, S. M., I. S. Kutiev, N. Jakowski, and S. Heise, Electron density profiles deduced from GPS TEC, O^+-H^+ transition height and ionosonde data, *Acta Geod. Geophys. Hung.*, *37*, 171–181, 2002.

N. Jakowski, S. Heise, and S. M. Stankov, Deutsches Zentrum für Luft- und Raumfahrt (DLR), Institut für Kommunikation und Navigation, D-17235 Neustrelitz, Germany. (Norbert.Jakowski@dlr.de; Stefan.Heise@dlr.de; Stanimir.Stankov@dlr.de)

I. Kutiev and P. Muhtarov, Bulgarian Academy of Sciences (BAS), Geophysical Institute, BG-1113 Sofia, Bulgaria. (ikutiev@geophys.bas.bg; pmuhtarov@geophys.bas.bg)

R. Warnant, Royal Observatory of Belgium (ROB), B-1180 Brussels, Belgium. (R.Warnant@oma.be)